Davidson College
Department of Biology

Honors Thesis

Title:

Constructing and Implementing a Transcription-Based XOR Gate in *Escherichia coli* through Promoter Engineering

Submitted by:

Will DeLoache
Class of 2009

Date of Submission:

April 6, 2009

FIRST READER: Dr. Malcolm Campbell

SECOND READER: Dr. David Wessner

Abstract

Synthetic biology is an emerging scientific field that utilizes biological principles to predictably engineer organisms to perform useful functions. In addition to holding great potential for solving real world problems, this multidisciplinary field offers valuable insight into specific areas where our understanding of biology is incomplete or wrong. Before complex systems can be engineered, it is important that simpler, well-characterized devices be developed. Towards that end, I have begun the construction of a modular XOR gate in *E. coli* that takes advantage of quorum-sensing transcription factors and promoter binding sites from *Pseudomonas aeruginosa* and *Vibrio fischeri*. This synthetic device was designed to perform XOR logic using two auto-inducer inputs to determine the transcriptional level of an interchangeable output gene. In addition to constructing this synthetic device, I also characterized a newly developed method for growing *E. coli* colonies in a time-delayed manner. Once the construction of the XOR gate promoters is completed, it will be possible to combine them with the time-delayed growth system to attempt to engineer a hash function in bacteria.

Introduction

Synthetic Biology

Recent advancements in DNA sequencing and synthesis technologies, along with increased understanding of biological systems, have opened the door for a new field of research commonly referred to as synthetic biology (Endy, 2005). Taking an engineering approach to biology, this expanding field attempts to rationally design and construct biological devices that perform useful functions. Building on traditional genetic engineering, which typically refers to the moving of a preexisting gene from one organism to another, synthetic biology seeks to utilize the concepts of abstraction and standardization to make possible the construction of larger, more complex genetic circuits (Anderson, 2008; Baker *et al.,* 2006). In addition to solving real world problems such as drug and energy production, the construction of novel gene circuits exposes gaps in our understanding of biology when well-designed devices fail to work as expected (Ferber *et al.,* 2004).

Currently, the synthetic biology community recognizes 3 abstraction levels that help to discretize synthetically designed systems into manageable pieces (Endy, 2005). "Parts" are small DNA elements that perform a basic biological function (i.e. a transcriptional terminator). Multiple parts can be assembled into a "device," which modularly performs some human-defined function (i.e. an AND logic gate). A "system", the highest abstraction level, is a combination of devices that performs a useful function and is typically not intended for further reuse (Endy, 2005).

Synthetic biologists have successfully constructed a wide range of simple biological devices, from a genetic ring oscillator that produces cyclical changes in fluorescent protein expression (Elowitz and Leibler, 2000), to a toggle switch that allows protein expression to be turned on or off based on environmental inputs (Gardner *et al.*, 2000). More recently, researchers have

3

attempted to scale up these devices into larger systems that have real world applications. In 2006, *Discover Magazine* named synthetic biologist Jay Keasling Scientist of the Year for his work engineering yeast to produce cheaper antimalarial drugs (Zimmer, 2006; Ro *et al.,* 2006). Others are working to make bacteria that fight cancer or produce renewable biofuels (Anderson, 2007; Baker *et al.,* 2006).

Bacterial Computation

For the past three years, synthetic biology research at Davidson College has centered on bacterial computation. In 2006, students working in the Campbell/Heyer Lab focused on engineering bacteria to solve the Burnt Pancake Problem *in vivo* (Haynes *et al.,* 2008). More recently, I was part of the 2007 iGEM team that developed a system to solve the Hamiltonian Path Problem using "living hardware" (Davidson/MWSU Hamiltonian Pathfinders, 2007; manuscript in preparation). Relying on living systems to perform computations, these projects fit into the broader category of information processing, one of the major branches of synthetic biology (Tan *et al.,* 2007).

Information processing in synthetic biology attempts to reconstruct natural systems into synthetic circuits to control how cells sense and respond to environmental changes. Efforts to construct such circuits have resulted in a collection of devices that can predictably control transcriptional and translational processes based on environmental inputs. Cellular memory (Gardner *et al.,* 2000; Kramer and Fussenegger, 2005; Ajo-Franklin *et al.,* 2007) and cellular logic gates (Kramer *et al.,* 2004; Anderson *et al.,* 2007; Win and Smolke, 2008) are two of the most well characterized types of synthetic circuits. However, the successful implementation of these simple devices into larger systems has seen very limited success. Lack of widespread success is due in part to our incomplete understanding of how their natural components

function *in vivo*, but also to a lack in device modularity.

My honors project was a continuation of the work performed by the 2008 Davidson College/Missouri Western State University iGEM (International Genetically Engineered Machines) team (Davidson/MWSU iGEM, 2008). Their project addressed two gaps in our knowledge of information processing in synthetic biology. Firstly, would it be possible to engineer a type of DNA-based logic that, to our knowledge, has eluded other labs. Secondly, I worked towards implementing this logic device in a larger system that could be useful in the real world. By bridging the gap between devices and systems, I hoped to address some of the challenges that exist both in the design of synthetic devices and the abstracting of engineered components for implementation in more complex systems.

Engineering an XOR Gate

The device that I attempted to engineer was a promoter-based exclusive-or (XOR) gate that responds to a pair of auto-inducer molecules (Table 1). Given the binary inputs A and B, XOR logic gates return true if A is true and B is false, or if B is true and A is false. Otherwise, the function returns false.

Input A	Input B	Output
0	0	0
1	0	1
0	1	1
1	1	0

Table 1: Truth Table of an XOR Logic Gate

While logic gates have been a popular area of synthetic biology research, a functional, *in vivo* XOR gate and its inverse, XNOR, have not been built from DNA parts. In 2004, Kramer *et al* described a collection of eukaryotic logic gates including NOT IF, AND, NOT IF IF,

NAND, OR, NOR, and INVERTER functions. This list includes all basic Boolean logic gates except XOR and XNOR. The inherent properties of XOR-type logic gates make them difficult to engineer in living cells. This type of logic requires that a cell respond differently to an input based solely on the presence or absence of a second input.

To engineer a genetic circuit that is capable of performing XOR logic, the 2008 iGEM team made use of two separate quorum-sensing systems from nature. The *lux* operon of *Vibrio fischeri* (Figure 1) is a well-characterized and commonly used system in synthetic circuits (Parts Registry, Cell-Cell Signaling; Waters and Bassler, 2005). In nature, the operon functions by secreting low levels of the autoinducer molecule 3OC6-homoserine lactone (3OC6; Figure 2). If enough cells are secreting 3OC6 in the same vicinity, 3OC6 will bind to and activate LuxR, a transcriptional activator of the *lux* operon. Activated LuxR causes increased transcription of LuxI which encodes an enzyme that produces more 3OC6, resulting in a positive feedback loop. In *Vibrio fischeri*, induction of this operon causes fluorescence via a luciferase protein that develops in squid as they age to help camouflage them while swimming (Waters and Bassler, 2005).
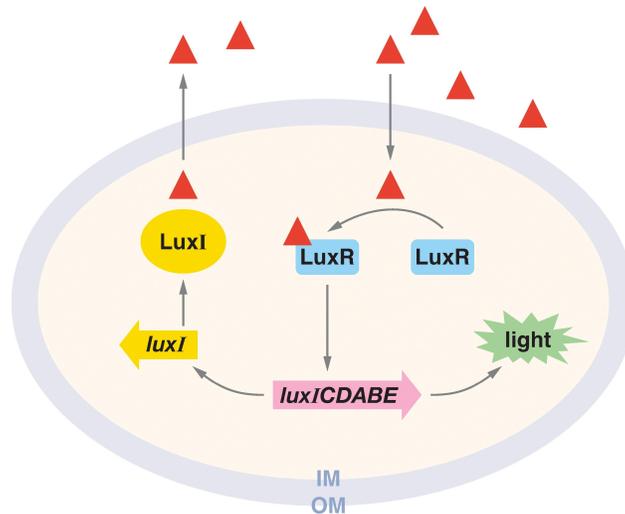
Figure 1: Quorum sensing in the *lux* operon. Red triangles represent 3OC6, which is produced by LuxI. (Figure extracted from Waters and Bassler, 2005).
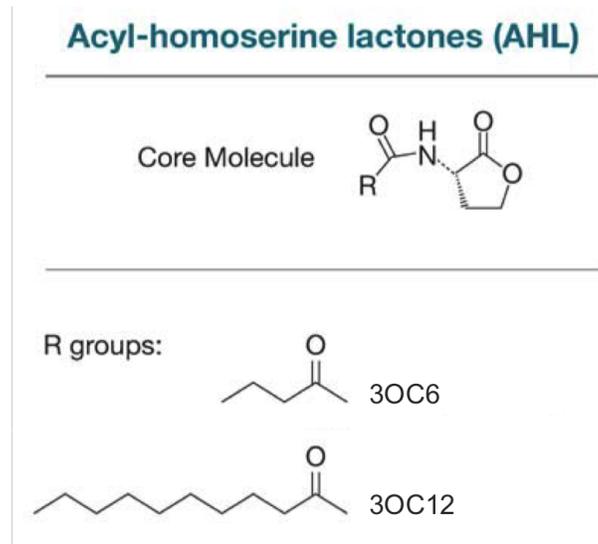
Figure 2: Structure of AHL autoinducer molecules. 3OC6 activates the *lux* system. 3OC12 activates the *las* system. (Figure adapted from Waters and Bassler, 2005).

Similar quorum sensing systems are used by various bacterial species, however, 3OC6-LuxR binding has been shown to be very specific, even in the presence of other quorum sensing molecules (Waters and Bassler, 2005). Therefore, the iGEM team utilized another quorum sensing system, the *las* system from *Pseudomonas aeruginosa*, as a complement to the *lux* system in the XOR gate. The *las* system works in the same way as the *lux* system, however, it responds to a distinct but related autoinducer molecule, 3OC12-homoserine lactone (3OC12; Figure 2). The proteins LasR and LasI are orthologs of LuxR and LuxI respectively.

Two new XOR promoters were designed using the binding sites from the wild type lux and las promoters (Figure 3). In its normal environment, the LuxR/3OC6 complex binds to the 20 bp *lux* box upstream of an inducible promoter, activating transcription. However, Egland and Greenberg (2000) showed that placing the *lux* box between the -35 and -10 consensus pLac promoter sequence caused the LuxR/3OC6 complex to function as a repressor instead of an activator. The 2008 iGEM team used the inversion of activation to design two hybrid inducible/repressible promoters. Each promoter carries one activation binding site as well

as one repression binding site that is specific to either the *las* or the *lux* system. In order to make the promoters solely responsive to the input of autoinducer molecules, LuxR and LasR would need to be constitutively expressed via a genomic insertion (Waters and Bassler, 2005).
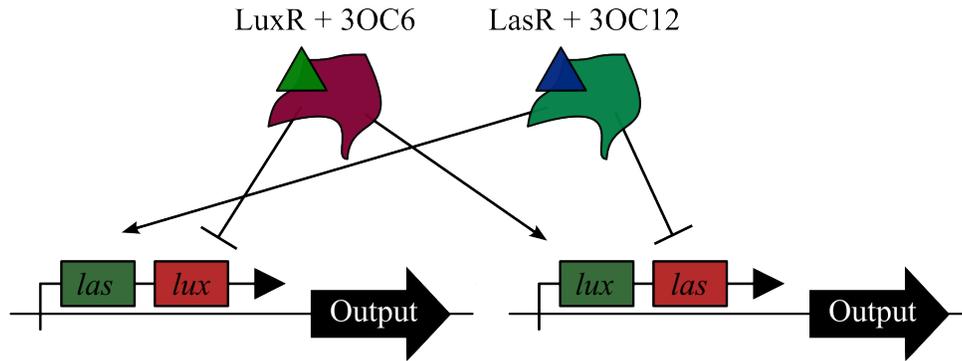
Figure 3: Design of XOR Gate. Each promoter contains two binding regions, one for activation (green box) and one for repression (red box). Promoter repression overrides activation. LuxR and LasR are constitutively expressed by the bacterial genome, and 3OC6 and 3OC12 are the two inputs to the system.

If neither 3OC6 nor 3OC12 is present in the cell, both promoters should be constitutively off since they lack the activation signal. If exactly one of the autoinducer molecules is present, one of the two promoters should be turned on and the other promoter should be repressed. If both autoinducers are present, then repression is expected to override activation, keeping both promoters off. In this way, XOR logic determines the transcriptional state of an output gene based on two molecular inputs.

Implementing a Simple Hash Function

An XOR gate could be applied to many types of larger systems, and our lab envisioned using it to implement a bacterial hash function. A hash function is a mathematical procedure that converts digital information of any length into a fixed-length "hash value." Hash functions

are used to obtain quick and easy access to large amounts of data by mapping a data-specific key to a distinct storage location. Hash functions also provide one-way encryption, in that the conversion of data into hash values is irreversible. Irreversibility makes hash functions a common method of password verification and secure-document validation (Mackenzie, 2008).

Recently, hash functions have received increased attention, as the need for newer and better hash algorithms has become evident (Mackenzie, 2008). As hash functions become more complex, the amount of computing power they require increases substantially. Therefore, the 2008 Davidson/MWSU iGEM team developed a bacterial hash function that could provide increased computing power through the parallel computing capabilities of bacteria (Figure 4; Haynes, 2008; Davidson/MWSU iGEM, 2008). I continued this work by preparing the XOR promoters for implementation in their system, by producing the transgenic *E. coli* to produce LuxR and LaxR, and by modeling a usable colony growth system.
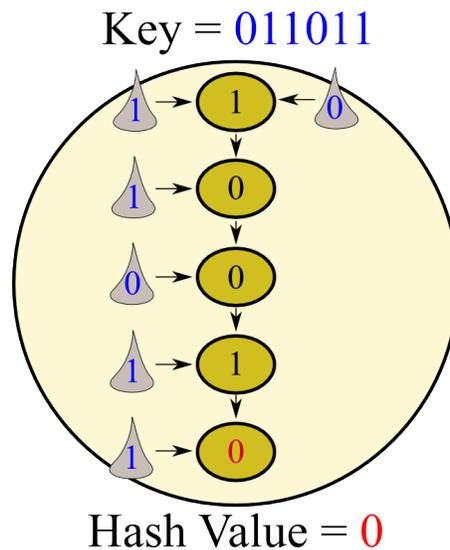
Figure 4: Bacterial Hash Function. Colonies (tan) will grow in a time-delayed manner. 3OC12 (left of the colonies) will be added manually to appropriate colonies. 3OC6 would come from preceding colonies that output a true value. Bacteria will respond with XOR logic to these inputs to determine whether or not to output 3OC6 to the next colony in the chain. The final colony in the chain will determine the hash value of the input (Figure adapted from Davidson/MWSU iGEM 2008).

To execute XOR logic as part of a bacterial hash function, the team wanted to place cells in

a row of colonies along an agar plate. The cells would carry the XOR gate promoters with LuxI as the output gene. If XOR logic produced LuxI, colonies would transmit 3OC6 to the next colony in the chain. Manual addition of 3OC12 to appropriate colonies would provide the system with a second input for the hash. If all cells grew simultaneously, the last colonies in the chain would grow and perform their XOR logic prior to receiving input from upstream colonies. Time-delayed growth of the colonies ensures that signals will move unidirectionally along the chain. This proof-of-concept hash function outputs a simple true/false hash value. However, more complex systems have been devised by the 2008 iGEM team that could scale this system up to output larger hash values, thus reducing the number of collisions that occur (Davidson/MWSU iGEM, 2008).

Time-Delayed Colony Growth

In order to implement a bacterial hash function with the XOR promoters, it will be necessary to have a system for time-delayed colony growth. Delayed growth will provide each colony time to process its inputs and respond with an output before the next colony in line can begin its own signal processing. To our knowledge, no solution to this problem has been presented in the literature, short of using microfluidics or other liquid handling procedures, which are in many cases expensive and unfeasible. A simple system that addressed time-delayed colony growth could be reused by other engineered systems that rely on molecular signals to be passed between cells. Several iGEM teams have hit the problem of time-delayed growth but not solved it (Brown University iGEM, 2006).

I attempted to develop and model a time-delayed growth system using a beta-lactamase-secreting colony on an LB agar plate containing ampicillin. Beta-lactamase is a protein that confers resistance to ampicillin and is known to diffuse through agar to allow growth of nearby cells called satellite colonies (OpenWetWare, Ampicillin). When performing transfor-

mations, satellite colonies are unwanted artifacts because they do not produce beta-lactamase themselves. Because ampicillin inhibits formation of the cell-wall, and therefore inhibits cell division, non-ampicillin resistant cells can survive on ampicillin media in the stationary phase until beta-lactamase has consumed all of the surrounding ampicillin. It is important to note that ampicillin, like many other antibiotics, does not kill *E. coli*.

I used the properties of ampicillin to my advantage to refine a time-delayed growth system. By placing a single beta-lactamase-secreting colony near multiple non-resistant colonies on an ampicillin plate, I hoped to quantify time-delayed growth of the non-resistant colonies as the beta-lactamase diffused through the agar (Figure 5). Colonies farther from the resistant colony grew later than colonies that are nearby, since the beta lactamase takes longer to diffuse out to those colonies. I tested and modeled delayed colony growth for three variables: ampicillin concentration, agar concentration, and growth temperature.
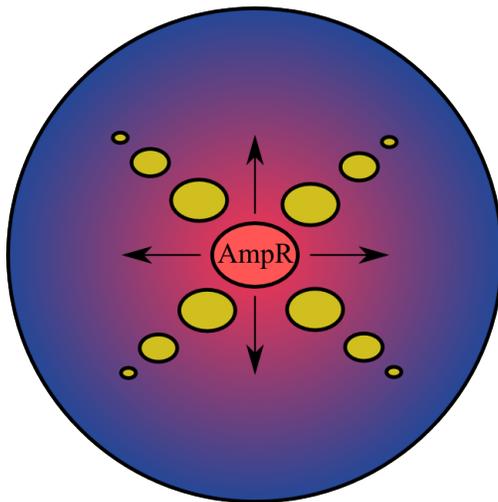
Figure 5: Time-delayed Growth. Beta-lactamase (red) is produced by the central colony, promoting growth of nearby, non-resistant colonies as it deactivates ampicillin (blue). Diffusion of beta lactamase through agar leads to time-delayed growth of non-resistant colonies.

Materials & Methods

Cell Strains: JM109 *E. coli* cells were used between rounds of BioBrick assembly. HB101 cells were initially used for the genomic insertion of the LuxR/LasR expression cassette (BBa_K091206). Upon failure of this construct into HB101, MC4100 *E. coli* cells were successfully cloned. Testing of the pLas' and pLasLux promoters occurred in this MC4100 derivative strain.

Bacterial cultures: Cells were grown in low salt Luria broth (LB) liquid culture or on LB agar plates. Ampicillin (100 ug/mL), gentamicin (20 ug/mL), and kanamycin (50 ug/uL) antibiotics were used to select for plasmid DNA.

Time-delayed Growth Experiments: Time-lapse images of the time-delayed cell growth system were taken over 3 days of growth at 32°C for the generation of a time-delayed growth movie. Images for this movie were taken with an Olympus fluorescent microscope under the control of ImagePro software. ImagePro was set to take a picture of the plate every 15 minutes. Images were compiled into a video file using ImageJ software.

A separate experiment was performed to gather further data on the effects of temperature (30°C and 37°C), agar concentration (7.5g/L, 15g/L, and 22.5g/L), and ampicillin concentration (25 μg/mL, 50 μg/mL, and 100 μg/mL) on cell growth rates. Images for this experiment were taken using BioRad gel imaging equipment every 2-12 hours for 3 days. Distances were measured using ImageJ by measuring from the ampicillin producing colony to the farthest-away non-resistant colony that was visible. Pixel lengths were then converted into distances based on calibration with a ruler.

Biobrick Standard Assembly: To assemble composite genetic parts, BioBrick standard part assembly was used (Knight, 2003). BBa standard plasmids (typically pSB1A2) containing an ampicillin resistance gene carried all basic parts. These parts are flanked by 4 standard restriction sites (EcoRI, XbaI, SpeI, and PstI) as shown in Figure 6. To assemble two parts, double digestion was performed on each plasmid so that when the products were mixed they would form a composite part. Either part can be inserted in front or behind the other part if the correct restriction enzyme pairs are used. The XbaI and SpeI sites have compatible sticky ends and form a 6 bp "mix site". Mix sites cannot be digested by any restriction enzyme so they are permanently ligated together. Composite parts can be used in future rounds of assembly.

Plasmid DNA Minipreps: Plasmid DNA minipreps were performed with the Promega Wizard Plus SV miniprep DNA purification system.
(`http://www.bio.davidson.edu/courses/Molbio/Protocols/miniprepPrmega.html`)

Measurement of DNA concentration: DNA concentrations were measured using a Nanodrop ND-1000.

DNA restriction enzyme digestions: Digestions were performed with Promega restriction enzymes and buffers. Buffers were selected based on the restriction enzyme combination.
(`http://www.bio.davidson.edu/courses/Molbio/Protocols/digestion.html`)
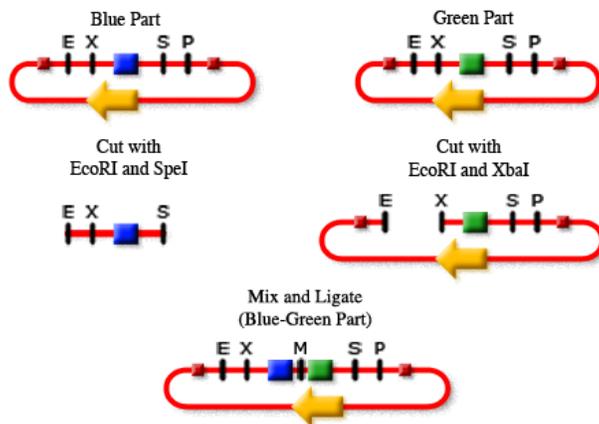
Figure 6: BioBrick Standard Assembly (Figure extracted from Knight, 2003).

Gel electrophoresis: Digested DNA was run on an agarose gel to separate products by length.
(`http://www.bio.davidson.edu/courses/Molbio/Protocols/pourgel.html`)
Optimal agarose percentages were calculated using a publicly available tool developed in the Campbell/Heyer Lab.
(`http://gcat.davidson.edu/iGEM08/gelwebsite/gelwebsite.html`)
DNA fragment length was estimated based on comparison with Invitrogen's 1Kb ladder.

DNA gel purification: The desired gel fragments were excised with a razor blade and purified using Quiagen's QiAquick gel extraction kit.
(`http://www.bio.davidson.edu/courses/Molbio/Protocols/Qiagen_gelpure.html`)

DNA ligation: Once the appropriate DNA fragments had been isolated from the digestion reaction, they were ligated using T4 DNA ligase and 2X rapid ligation buffer.
(`http://www.bio.davidson.edu/courses/Molbio/Protocols/ligation.html`)

Z-competent cell transformations: Plasmid DNA was typically transformed into Zymo's Zippy Z-competent cells (JM109 strain). If the selectable antibiotic was not ampicillin, the cells were first rescued in LB for 1 hour. The transformed cells were then spread on LB agar plates containing the appropriate antibiotic.
(`http://www.bio.davidson.edu/courses/Molbio/Protocols/Zippy_Transformation.html`)

Chemically competent cell transformations
Chemically competent cell transformations were also performed using various cell strains grown to mid-log and then heat shocked in TSS buffer. Again, if the selectable antibiotic was not ampicillin, the cells were first rescued in LB for 1 hour. The transformed cells were then spread on LB agar plates containing the appropriate antibiotic.
(`http://gcat.davidson.edu/GcatWiki/index.php/Competent_Cells_-_Small_Scale`)

Colony PCR screen for successful ligation: After each round of BioBrick assembly,

multiple colonies from the transformation plate were PCR screened for successful ligations. Primers VF2 and VR bound upstream and downstream of the BioBrick restriction sites and amplified the part contained by the plasmid. Successful ligations were confirmed by running the PCR reaction on a gel and verifying that products were the same length as the expected composite part. Minipreps were performed on PCR-positive colonies. (`http://www.bio.davidson.edu/courses/Molbio/Protocols/ColonyPCR_Screening.html`)

Primer VF2 (Forward Primer): 5'-TGCCACCTGACGTCTAAGAA-3'

Primer VR (Reverse Primer): 5'-ATTACCGCCTTTGAGTGAGC-3'

Preparation and transformation of chemically competent cells: When cell strains other than JM109 were needed for plasmid transformations, chemically competent cells were prepared. (`http://gcat.davidson.edu/GcatWiki/index.php/Competent_Cells_-_Small_Scale`)

XOR promoter design:

The sequences of the XOR promoters are shown below. Included are the sequences of control promoter constructs (pLux' and pLas') that only include the activator binding region. Wild type pLux and pLas sequences were modified to arrive at these designs. In each construct, the _lux_ box is underlined twice and the _las_ box is underlined once. The **-35** and **-10** promoter regions are shown in bold. A single thymine was removed from the 3' end of the consensus _las_ box to avoid interference with the spacing between the -35 and the -10 consensus regions of the promoters. The pLas' promoter was designed to control for this deletion.

pLux' (BBa_K091156):

5'-acctgtaggatcgtacagg**ttgaca**tcaagaaaatggtttgt**tataat**cg
aataaA-3'

pLuxLas (BBa_K091157):

5'-acctgtaggatcgtacagg**ttgaca**tctatctcatttgctag**tataat**cga
ataaa-3'

pLas' (BBa_K091117)

5'-tgttctcgtgtgaagccattgctctgatcttttggacgtttcttcgagcct
agcaagggtccgggttcaccgaaatctatctcat**ttgctag**ttataaaattatgaaatttg**tataaa**ttcttcag-3'

pLasLux (BBa_K091146)

5'-tgttctcgtgtgaagccattgctctgatcttttggacgtttcttcgagcct
agcaagggtccgggttcaccgaaatctatctcat**ttgctag**tacctgtaggatcgtacagg**tataaa**ttcttcag-3'

XOR promoter construction: The pLas' and pLasLux promoters were assembled by oligonucleotide assembly by the iGEM team. The pLux' and pLuxLas promoters were synthesized by GeneArt after multiple unsuccessful in-house attempts to construct mutation-free promoters through oligonucleotide assembly and primer dimer assembly.

Oligonucleotide Assembly:

(http://www.bio.davidson.edu/courses/Molbio/Protocols/anneal_oligos.html)

pLux' Oligonucleotide Sequences:

31-mer 5'-AATTCGCGGCCGCTTCTAGAGACCTGTAGGA-3'
66-mer 5'-TCGTACAGGTTGACATCAAGAAAATGGTTTGTTATAATCGAATAA
ATACTAGTAGCGGCCGCTGCA-3'
tab 60-mer 5'-AACAAACCATTTTCTTGATGTCAACCTGTACGATCCTACAGG
TCTCTAGAAGCGGCCGCG-3'
29-mer 5'-GCGGCCGCTACTAGTATTTATTCGATTAT-3'

pLuxLas Oligonucleotide Sequences:

31-mer 5'-AATTCGCGGCCGCTTCTAGAGACCTGTAGGA-3'
66-mer 5'-TCGTACAGGTTGACATCTATCTCATTTGCTAGTATAATCGAATAA
ATACTAGTAGCGGCCGCTGCA-3'
60-mer 5'-ACTAGCAAATGAGATAGATGTCAACCTGTACGATCCTACAGGTC
TCTAGAAGCGGCCGCG-3'
29-mer 5'-GCGGCCGCTACTAGTATTTATTCGATTAT-3'

Oligonucleotide design web site for Primer Dimer Assembly:

(http://openwetware.org/wiki/Knight:Annealing_and_primer_extension_with_Taq_pol
ymerase)

pLux' Primer Sequences:

Forward Primer: 5'-GCATgaattcgcggccgcttctagagACCTGTAGGATCGTACAG
GTTGACATCAAGAAAAT GGT-3'
Reverse Primer: 5'-GCATCTGCAGCGGCCGCTACTAGTATTTATTCGATTAT
AACAAACCATTTTCTTGATGTCAAC-3'

pLuxLas Primer Sequences:

Forward Primer: 5'-GCATGAATTCGCGGCCGCTTCTAGAGACCTGTAGGAT
CGTACAGGTTGACATCTATCTCATTTG-3'
Reverse Primer: 5'-GCATCTGCAGCGGCCGCTACTAGTATTTATTCGATTAT
ACTAGCAAATGAGATAGATGTCAAC 3'

Genomic integration: To perform the genomic integration of the LuxR/LasR expression cassette (BBa_K091206), I used conditional-replication, integration, and modular (CRIM) plasmid technology (Haldimann and Wanner, 2001). The protocol I followed was adapted from a modified CRIM protocol as developed in the Anderson Lab at UC Berkeley. (http://gcat.davidson.edu/GcatWiki/index.php/Genomic_Insertion_Protocol)

Genomic integration PCR verification primer sequences:

attPhi80-1 (Verification Primer 1): 5'-CTGCTTGTGGTGGTGAAT-3'

attPhi80-2 (Verification Primer 2): 5'-ACTTAACGGCTGACATGG-3'

attPhi80-3 (Verification Primer 3): 5'-ACGAGTATCGAGATGGCA-3'

attPhi80-4 (Verification Primer 4): 5'-TAAGGCAAGACGATCAGG-3'

PCR Reactions with Various Primers	Expected Band Lengths (bp)
No Integrant with 1/4	546
Single Integrant with 1/2, 3/4	409, 732
Multiple Integrants with 1/2, 3/4, 1/4	409, 595, 732

Table 2: Expected PCR product lengths for 0, 1, or >1 genomic insertion events.

Fluorescence Measurements:
Cell fluorescence was measured in 96-well plates using an FLx800 Microplate Fluorescence Reader (excitation: 485/20 nm, emission: 528/20 nm) and a Bio-Tek ELx808 Optical Density Reader (595 nm). KC Junior software was used to collect and analyze the results. Cell cultures were grown in LB+antibiotics to saturation and then diluted 1:20 into 200uL of LB+antibiotic in 96 well plates. Cells were then allowed to incubate for 20 hours at 37°C before taking fluorescence measurements. Fluorescence measurements were divided by optical density readings to reduce the effects of differences in the number of cells in the culture.

3OC6 was ordered from Sigma Aldrich (#K3007). 3OC12 was ordered from Cayman Chemicals (#10007895). A stock solution of each autoinducer molecule (10 mg in 1 mL EtOH) was prepared and kept at -20°C to prevent the EtOH from opening the lactam rings. Both autoinducer molecules were added at an optimal concentration of 10^{-5} M. This concentration was determined by performing a serial dilution of the autoinducer molecules and measuring fluorescence at each concentration. It should be noted that this concentration differs from that found in the literature (Pearson *et al.,* 1994 and MIT Parts Registry, BBa_F2620: Transfer Function).

Lab Notebook:
I maintained an online lab notebook on our lab's local wiki. This notebook is openly available to everyone and contains additional data, protocols, and day-to-day discussion of my results. It can be accessed here:
(http://gcat.davidson.edu/GcatWiki/index.php/Will_DeLoache_Notebook)

Results

Building the pLux' and pLuxLas Promoters

Construction of the XOR gate promoters began during the summer of 2008. The pLasLux promoter (which is activated by LasR+3OC12 and repressed by LuxR+3OC6) and its con-

trol promoter, pLas', were constructed by the 2008 Davidson iGEM team via oligonucleotide assembly. These promoter parts were entered into the MIT Parts Registry (pLasLux: BBa_K091146, pLas': BBa_K091117) and ligated upstream of an RBS_GFP expression cassette (BBa_E0240). The pLux' and pLuxLas promoters proved more difficult to construct, however. Over the summer, the Davidson iGEM team had attempted construction of the parts via primer dimer assembly but this attempt resulted in mutations in all promoter constructs sequenced. The team concluded that the oligonucleotides were synthesized with mutations.

I began construction of the pLux' and pLuxLas promoters by ordering new oligonucleotides and attempting primer dimer assembly of the two pLux promoter parts. I used a different protocol than was used over the summer. The modified protocol requires five rounds of amplification instead of 30 to minimize the chances of mutation during amplification. Based on a digestion of the resulting DNA preps, I had 3 pLuxLas clones that appeared to have the correct length insert and no pLux' clones that were the correct length (Figure 7).
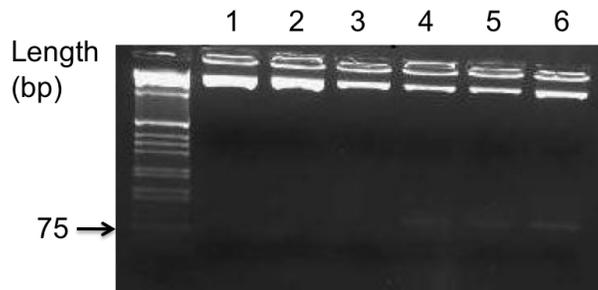
Figure 7: EcoRI and PstI digestion of cloned pLux' and pLuxLas primer dimer assemblies (2.2% gel). Expected length of all promoter parts = 94 bps. Lanes 1-3 are 3 pLux' clones, showing no visible insert near the expected length. Lanes 4-6 are 3 pLuxLas clones, showing the expected insert length.

I sequenced the three pLuxLas clones to see if any of them were the correct part. Unfortunately, all sequences came back with at least one mutation (Figure 8). Clone 1 has a single mutation, while clones 2 and 3 have multiple. Each clone had unique mutations which

17

indicates the PCR did not amplify a single mutation.

```
Expected    GAATTCGCGGCCGCTTCTAGAGACCTGTAGGATCGTACAGGTTGACATCTATCTCATTTGCTAGTATAATCGAATAAATACTAGTAGCGGCCGC 94
1           GAATTCGCGGCCGCTTCTAGAGACTTGTAGGATCGTACAGGTTGACATCTATCTCATTTGCTAG-ATAATCGAATAAATACTAGTAGCGGCCGC 93
2           GAATTCGCGGCCGCTTCTAGAGACCTGTAGGATCGTACAGGTTGACATCTATCTCATTTGCTAGTATA-TCGAATAAA-ACTAGTAGCGGCCG- 91
3           GAATTCGCGGCCGCTTCTAGAGACCTGTAGGATCGTACAGGTTGACATCTATCTCATTTGCTAGTAAA-TCGAATAAATACTAGTAGCGGCCG- 92
            ************************ *************************************** * * ********* *************
```

Figure 8: ClustalW sequence alignment of all 3 pLuxLas sequences with the expected sequence. Asterisks (*) denote positions with agreement across all sequences. No sequences match the expected sequence and no mutation occurs in all 3 pLuxLas clones.

Because the primer dimer assembly had failed to work even with the modified protocol, I decided to try oligonucleotide assembly as an alternative method of assembling the pLux promoter constructs. Two consecutive attempts to assemble the pLux promoters from 4 overlapping oligonucleotides resulted in failure. On the first attempt, all of the isolated plasmids retained the 800bp irrelevant insert that I had tried to remove from the plasmid prior to oligonucleotide assembly. The second attempt yielded no colonies for either the pLux' or the pLuxLas promoters. This protocol had been used many times in the lab, so the failure to obtain colonies was surprising.

After so many failed attempts to construct these parts in our lab, it was decided to have the two promoters synthesized by GeneArt along with two other constructs needed for other projects going on in the lab. These other parts were named LacI-I12X86 and LacI-X86. To save on gene synthesis costs, my pLux promoters were synthesized downstream of the two other constructs, resulting in the two plasmids shown in Figure 9 that were shipped from GeneArt.

Based on this sequence map, I performed two digestions on the plasmids from GeneArt: one with EcoRI alone and the second with EcoRI and PstI (Figure 10). All of these digestions gave the expected band lengths, suggesting that the plasmids were correct. I, therefore, gel purified the EcoRI-PstI bands at 93 bps, the expected size for the pLux' and pLuxLas engineered promoters. These fragments are marked in red boxes in Figure 10. These two

(a) LacII12X86-pLuxLas   (b) LacIX86-pLux'
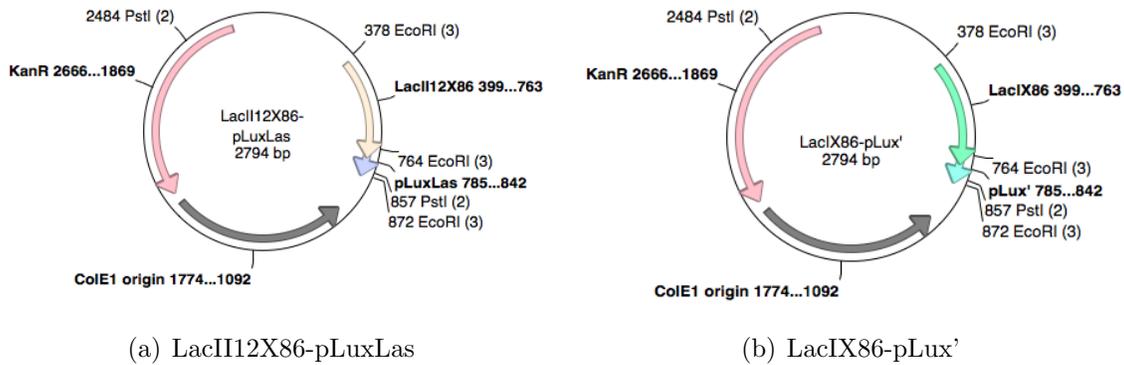
Figure 9: pLuxLas (left) and pLux' (right) in the plasmids shipped from GeneArt. EcoRI and PstI sites are denoted. The XOR promoters appear as small arrows around 4 o'clock on the plasmid diagram.

parts were ligated into a standard assembly vector, pSB1A2.
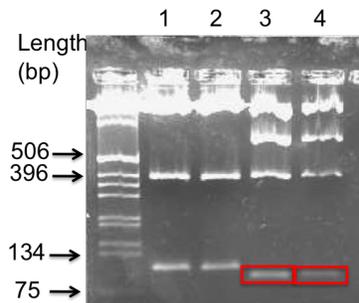
Figure 10: pLux' and pLuxLas plasmid digestions from GeneArt (2.0% gel). Lanes 1, 2: EcoRI digestions. Lanes 3,4: EcoRI/PstI digestions. Lanes 1, 3: pLux' plasmid. Lanes 2, 4: pLuxLas plasmid. Expected size for pLux promoters with EcoRI digestion = 108 bp. Expected size for pLux promoters with EcoRI/PstI digestion = 93 bp. Bands marked in red boxes were excised for ligation with pSB1A2.

I purified plasmid DNA from 3 colonies from each transformation plate and digested the samples with EcoRI and PstI. Upon running these digestions on a gel, I found that 5 of the 6 clones were religations of the 800 bp part that I had attempted to cut out of pSB1A2 prior to ligation (Figure 11). There was one pLuxLas clone that appeared to be the correct length (lane 5, 93 bp), although the band at this length was very faint. At the very least, the part was certainly different from the other 5 clones, so I moved forward hoping that I

19

had successfully cloned pLuxLas.
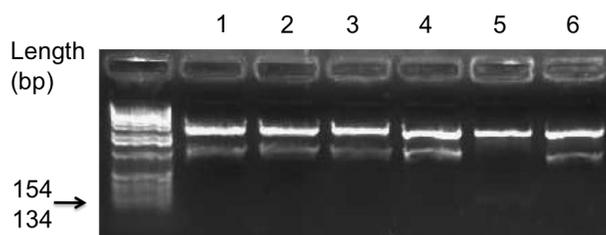
Figure 11: EcoRI and PstI digestions of potential pLux' and pLuxLas clones (0.8% gel). Lanes 1-3: pLux' clones. Lanes 4-6: pLuxLas clones. A faint band can be seen around 100 bps in lane 5. Expected length of band from successful ligation = 93 bps. I proceeded using the pLuxLas clone from lane 5.

Since I did not find pLux' in the first 3 colonies, I did a PCR colony screen of 7 additional colonies from the transformation plate of this construct (Figure 12). I used the successfully cloned pLuxLas as a control for the expected length of a successful ligation. This resulted in 2 potential clones that contained a successful ligation, in lanes 1 and 7, both of which appeared to match the length of the pLuxLas control in lane 8. All other lanes either failed to give a PCR product or gave a product that was too long. I proceeded using the pLux' clone from lane 7, thinking that I now had both pLux' and pLuxLas cloned into pSB1A2.
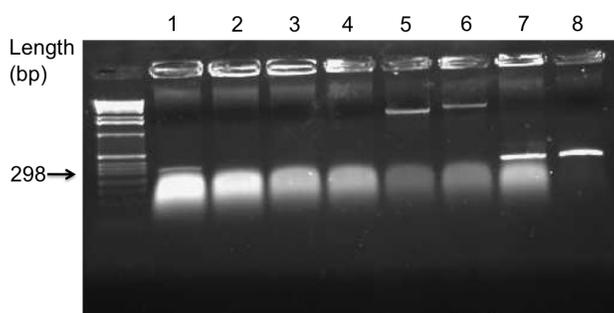
Figure 12: PCR colony screen of potential pLux' clones (1.0% gel). Lanes 1-7: pLux' clones. Lane 8: pLuxLas positive control for successful ligation. Expected length of the PCR product = 294 bp.

I ligated a GFP expression cassette (BBa_E0240) behind the pLux' and pLuxLas promoters. Unfortunately, multiple attempts at this ligation yielded very high levels of colonies on

20

my negative control plate (no GFP insert added to the ligation). This reproducible result suggested that my SpeI/PstI digestions of the pSB1A2-pLux were not digesting completely (making it possible for the plasmid to religate onto itself even after a gel purification). Therefore, I decided to sequence the two promoter parts to ensure that the SpeI site was in the correct location. I used the reverse primer VR for sequencing of both parts.

The results of this sequencing reaction were not what I expected at all. I found that, while the EcoRI and PstI sites were intact, the DNA inserts between them were not correct at all. Neither the putative pLux' or the pLuxLas clone contained XbaI or SpeI sites between the EcoRI and PstI sites, as is true for all BioBrick standard parts. These unexpected sequences meant that I had ligated something other than the promoters into the pSB1A2 plasmids. The pLux' and pLuxLas promoters should be 87 bps between the EcoRI and PstI sites. The sequencing showed that the putative pLux' clone was 104 bps and the putative pLuxLas clone was 88 bps in this region. The difference between these lengths is too small to resolve on an agarose gel. However, neither insert was close to the intended modified pLux promoter.

I investigated further what the possible source of these inserts could be by BLASTing them against the NCBI database. The pLux' sequence showed no hits with the database, while the pLuxLas found nearly a perfect match (including the EcoRI and PstI sites) in the *E. coli* genome (Figure 13). This result suggested that genomic DNA must have been in the prep sent by GeneArt. Upon digestion of this prep with EcoRI/PstI, I inadvertently purified and ligated a genomic fragment in addition to the pLuxLas promoter part. Needless to say, cloning genomic DNA should have been a very unlikely event. Unfortunately, at this point in the semester, I was out of time and could no longer investigate the possible causes for this strange set of cloning mishaps.

```
>gb|CP000948.1| D Escherichia coli str. K12 substr. DH10B, complete genome
Length=4686137

 Features in this part of subject sequence:
    predicted DNA-binding transcriptional regulator

 Score =  182 bits (98),  Expect = 3e-43
 Identities = 99/100 (99%), Gaps = 0/100 (0%)
 Strand=Plus/Minus

Query  1        CTGCAGAGTCAAACTGACATGTTTCNTTTTTCCCGTTCCAGGCATTTTAATTCCTTCGCG  60
                ||||||||||||||||||||||||| |||||||||||||||||||||||||||||||||||
Sbjct  1608925  CTGCAGAGTCAAACTGACATGTTTCATTTTTCCCGTTCCAGGCATTTTAATTCCTTCGCG  1608866

Query  61       TGTTTTCTGTCCAACCCTGCCTGCATGGCAGAAGGAATTC  100
                ||||||||||||||||||||||||||||||||||||||||
Sbjct  1608865  TGTTTTCTGTCCAACCCTGCCTGCATGGCAGAAGGAATTC  1608826
```

Figure 13: Screen shot of NCBI BLAST results for the pLuxLas sequence. The pLuxLas sequencing results from (and including) the EcoRI and PstI sites were blasted. A 99% match was found between the sequencing results and the *E. coli* genome (K12 strain in this case).

Genomic Insertion of the LuxR/LasR Expression Cassette

As I was attempting to clone the pLux promoters, I was also working on engineering transgenic *E. coli* that constitutively expressed both LuxR and LasR, which are necessary for autoinducer signalling. To do this, I constructed a plasmid-based LuxR/LasR expression cassette which I inserted into the *E. coli* genome. The cassette consisted of two copies of a constitutive promoter upstream the *luxR* and *lasR* genes. Each gene was followed by a transcriptional terminator. This part was entered into the BioBrick parts registry with the number BBa_K091206 (Figure 14). Once I had completed multiple rounds of ligation (not shown) and verified that a successful expression cassette had been built (Figure 15), I was ready to perform the genomic integration of this part.

J23100 B0034 C0062 B0010/12   J23100 B0034 C0079 B0010/12

pCon RBS luxR T.T.   pCon RBS lasR T.T.
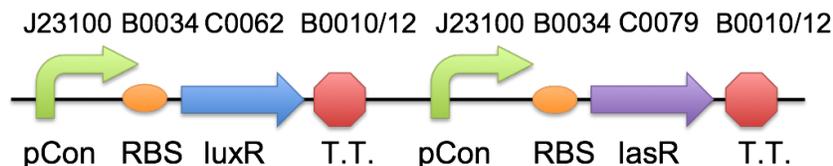
Figure 14: LuxR/LasR Expression Cassette (BBa_K091206). Part registry numbers are given above the symbols. Descriptions are shown below. This cassette was inserted into the *E. coli* genome to provide constitutive expression of LuxR and LasR.
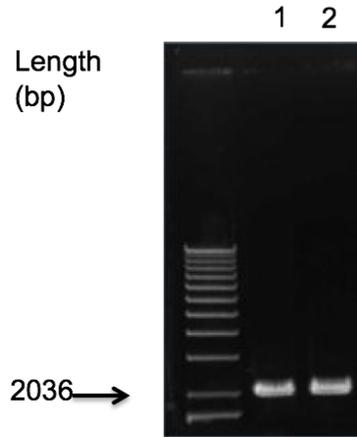
Figure 15: EcoRI and PstI digestion of pSB1A2-K091206 minipreps for verification of successful assembly (0.4% gel). Expected length for K091206 = 2003bp. Expected length for vector = 2042bp. Both samples appeared to have the correct size bands. However, it was impossible to resolve the two bands for gel purification of K091206.

The procedure for genomic integration was new to our lab so I will describe the method in this section. The basic procedure relies on two conditional-replication plasmids (Haldimann and Wanner, 2001). The first, pG80ko, contains the R6K origin of replication, which is only active in the presence of Pir protein (Figure 16). A second helper plasmid, pInt80-649, can only be replicated inside the cell at temperatures below 43°C because the CI857 protein, which is necessary for replication, is inactivated at high temperatures (Figure 17). In order to perform a genomic insertion, the DNA to be inserted is placed on pG80ko. This plasmid is transformed into cells that already contain pInt80-649 (and thus express Pir). PG80ko carries a Φ80 attP site that allows for recombination with the Φ80 attB site in the *E. coli* genome. This recombination event is aided by the integrase which is expressed by the helper plasmid, pInt80-649.

Cells that have undergone a recombination event can be selected by growth on gentamicin plates at 43°C. High temperatures cause the cells to stop replication of the helper plasmid and consequently stop production of Pir too. Without Pir, pG80ko is incapable of replication
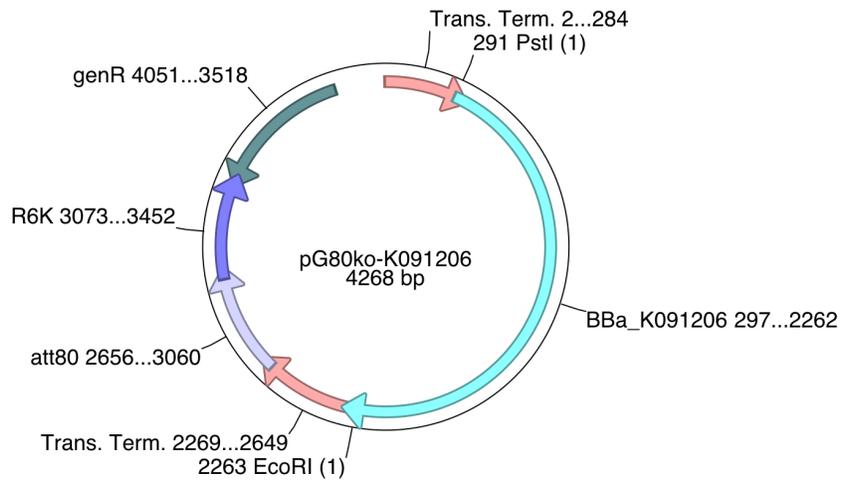
Figure 16: Integration plasmid pG80ko with LuxR/LasR expression cassette (BBa_K091206). The R6K origin requires Pir expression for replication. Genomic integration occurs via a recombination event between the plasmid's att80 site and the Φ80 site on the *E. coli* chromosome. The plasmid is insulated with two transcriptional terminators to prevent read-through transcription once in the genome.
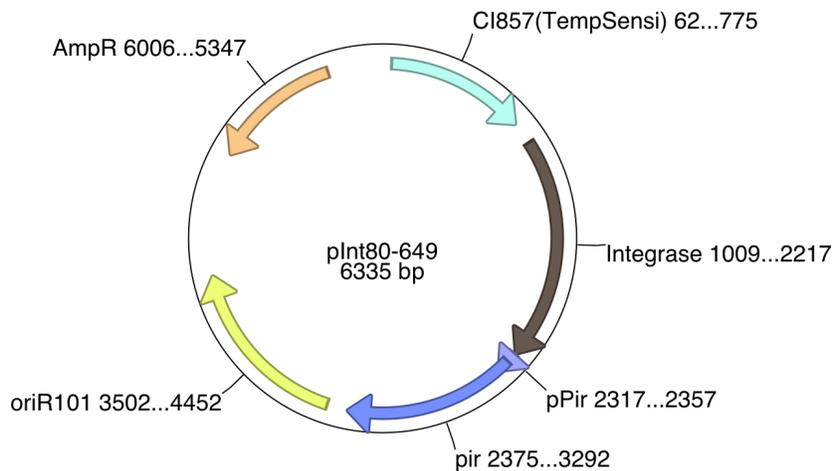
Figure 17: Helper plasmid pInt80-649. When present in the cell, the helper plasmid expresses *pir* and allows for replication of pG80ko. When exposed to 43°C temperatures, CI857 becomes inactive and pInt80-649 cannot be replicated. Curing cells of the helper plasmid also cures them of the insertion plasmid. Therefore, only cells that have undergone a genomic insertion can survive gentamicin selection at 43°C.

and cells that have not undergone integration lose their resistance to gentamicin. At 43°C, only transgenic cells should express a gentamicin resistance gene. Genomic integration is verified by PCR near the Φ80 integration site on the *E. coli* chromosome. As specified by Haldimann and Wanner (2001), 4 primers allowed me to distinguish between a single and multiple integration events (Materials and Methods, Table 2).

I used this basic framework to integrate K091206 into the *E. coli* genome. First, I needed to clone K091206 into pG80ko using an EcoRI/PstI restriction digest and ligation. Unfortunately, the difference in fragment length between K091206 and the pSB1A2 vector in which it resided was only 39 bps when digested with EcoRI/PstI. This difference was too small to resolve on a gel, as can be seen in Figure 15.

In order to move K091206 into pG80ko, I searched for a unique restriction site somewhere in the middle of pSB1A2 vector. Luckily, there was a ScaI site and by doing a triple digestion of the pSB1A2-K091206 plasmid (EcoRI, ScaI, and PstI), I was able to cut the vector into 1492 bp and 550 bp fragments. The bands resolved nicely once the vector was cut in two pieces (Figure 18). I transformed the ligation of K091206 and pG80ko into Ec100D::pir+ cells that had been sent from the Anderson Lab at UC Berkeley. These cells constitutively expressed pir protein and made replication of the pG80ko plasmid possible. I picked two colonies from the transformation and verified for successful ligation (Figure 19).

The final step to the genomic insertion was the cotransformation of the helper plasmid, pInt80-649, and the integration plasmid into the target strain. The paper by Haldimann and Wanner indicated a wide range of strains were suitable for this method. We chose HB101 cells as the strain to receive the genomic insertion because another student in the lab was working on a different project in this cell strain and it does not have a LacI gene which might affect future projects. The transformations were performed in succession, with the helper plasmid, pInt80-649, being transformed in first so that pir expression could begin before
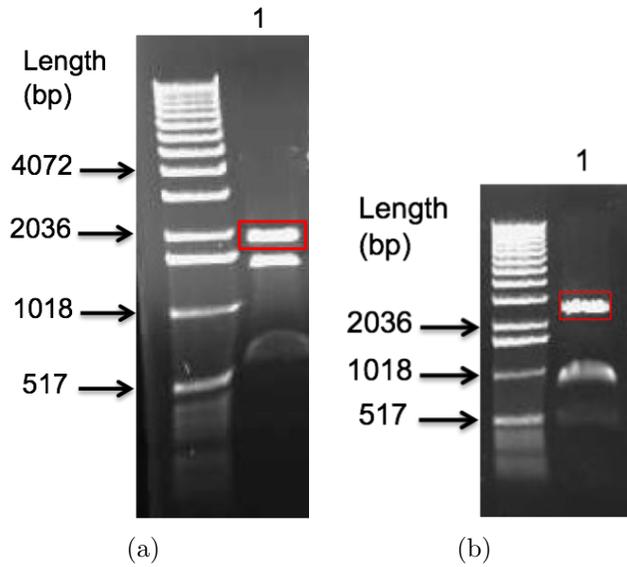
Figure 18: Gel fragments that were excised to construct pG80ko-K091206. The gel in panel a (0.4%) shows the triple digestion (EcoRI/PstI/ScaI) of pSB1A2-K09120. Expected band lengths were: K091206 = 2003 bps, Vector = 1492 and 550 bps. The gel in panel b (0.4%) shows the EcoRI/PstI digestion of pG80ko. The expected size of the pG80ko vector was 2296 bp. The insert in pG80ko was unknown because the plasmid was shipped from the Anderson Lab in Berkeley. The bands with red squares around them were excised and ligated together.
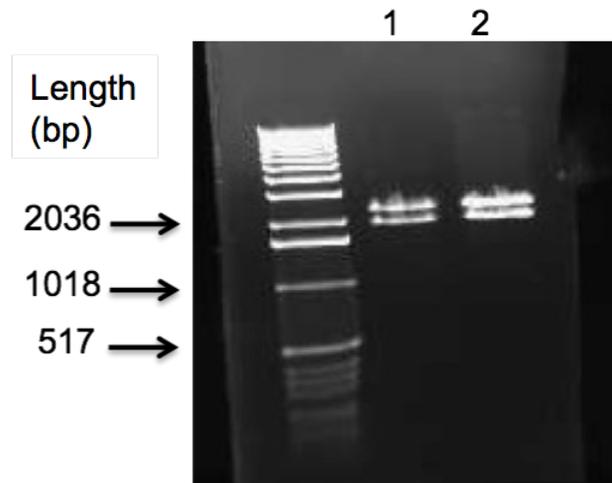
Figure 19: Figure 19: EcoRI and PstI digestion of pG80ko-K091206 minipreps for verification of successful ligation (0.6% gel). Expected lengths were: K091206 = 2003 bps, pG80ko = 2296 bps. Both samples appeared to be correct, so I moved on using the sample from lane 1 for future manipulations.

transformation of the integration plasmid. All growth manipulations on cells containing the temperature sensitive plasmid were done at 30 °C. Strangely, these cells took almost 3 days to appear on the plate. Slow growth may have been an indication that the cells were unstable, however, I proceeded to the transformation of the integration plasmid into the HB101 + pInt80-649 cells and plated on a gentamicin plate.

After another 3 days of growth at room temperature, colonies finally appeared on this plate. I picked a colony and grew it up in liquid culture overnight. I streaked this culture on gentamicin plates at 43°C and 30°C, but I only observed growth at 30°C. This would have been the final step of the genomic integration. Because I didn't get growth at 43°C, I purified plasmid DNA from the cotransformed HB101 cells and digested it with EcoRI to validate that both plasmids were in the cells (Figure 20). While this digestion showed some extra products at unexpected lengths, bands did appear at the expected positions for both the integration and the helper plasmid. Bands of unexpected length were not completely inexplicable, as genomic recombination events theoretically should have been occurring in these cells.

Because the doubly transformed HB101 cells failed to grow at 43°C after multiple iterations of this experiment, I began to suspect that the cell strain was the source of my problems. To test this suspicion, I decided to do the integration procedure in both HB101 and MC4100 cells in parallel. MC4100's were chosen because they are a closer to wildtype K12 *E. coli* than HB101. When I performed the second transformation step with MC4100 and HB101 cells in parallel, I found that the HB101 cells yielded no colonies, while the MC4100 transformation plate contained 7 colonies (Figure 21). These results suggested that some difference existed between the HB101 and MC4100 cells in terms of their ability to maintain both plasmids. Strangely, no colonies appeared on the HB101 cells after >4 days at room temp, unlike my previous results.
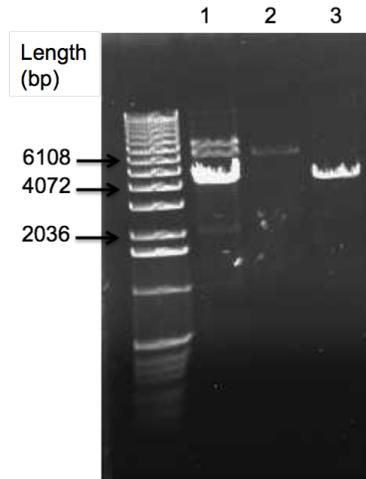
Figure 20: Verification of cotransformation in HB101 cells (0.4% gel). Lane 1 contains a miniprep of the HB101 cells digested with EcoRI (expected lengths = 6335 and 4268 bps). Lane 2 contains pInt80-649 digested with EcoRI (expected length = 6335 bps). Lane 3 contains pG80ko-K091206 digested with EcoRI (expected length = 4268 bps). While unexpected bands appear at 7000 and 2000 bps, both pInt80-649 and pG80ko-K091206 appear to be present in the miniprep.
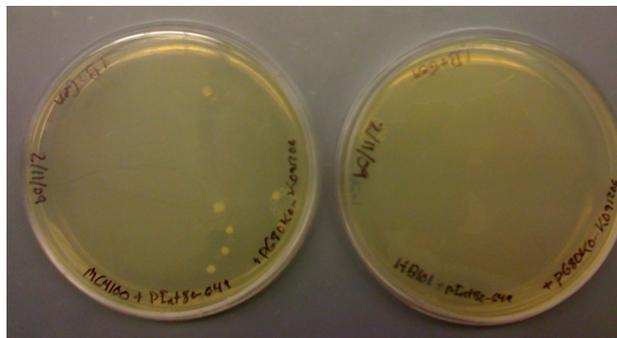
Figure 21: Transformation of pG80ko-K091206 into MC4100 (left) and HB101 cells containing pInt80ko-649. LB+Gentamicin plates.

When I picked one of the MC4100 colonies, grew it up at 37°C, and streaked at 43°C, I finally had a plate full of gentamicin resistant colonies. I performed a PCR screen of a colony from this plate to test for a successful genomic insertion using the 4 PCR primers described by Haldimann and Wanner (2001; Figure 22). I included PCR's of MC4100 + pInt80-649 cells and of the integration plasmid alone as controls.
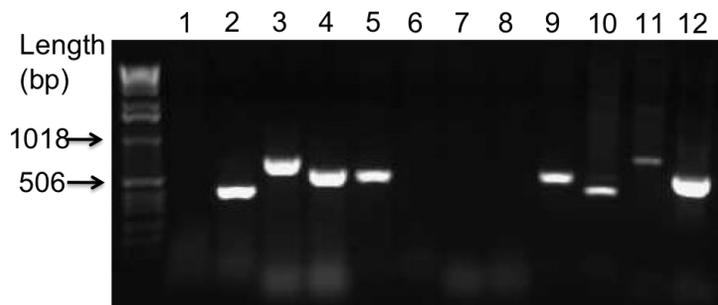
Figure 22: Colony PCR to verify successful genomic integration of pG80ko-K091206 into MC4100. Lanes 1-4: MC4100 + pInt80-649 + pG80ko-K091206 from 43°C plate. Lanes 5-8: MC4100 + pInt80-649. Lanes 9-12: pG80ko-K091206. attPhi80 primers were used in the following combinations from left to right for each template: 1/4, 1/2, 3/4, 3/2. Lanes 1-8, 12 suggested a successful integration (see Materials and Methods for expected band lengths). Bands in lanes 9-11 were unexpected. A band in lane 4 suggests that multiple copies of the integrant were inserted into the genome.

The PCR results I obtained were, in general, as expected for a successful integration event with a couple of exceptions. While primers 1/4 gave a 546 bp band for wild-type MC4100 cells, the absence of a band with these primers in the transgenic MC4100 cells is consistent with successful integration at the phi80 site because an integrated plasmid would increase the distance between the primers by >4000 bps and thus would not amplify with the short elongation step of my PCR. Additionally, other primer combinations gave the expected band lengths for a transgenic strain with multiple integrants as documented by Haldimann and Wanner (2001). Unexpected bands appeared for the pG80ko-K091206 plasmid in lanes 9-11, but I had sufficient evidence to suggest a genomic integration had occurred (This will be addressed in the discussion section). I called this new transgenic strain MC4100::K091206.

Fluorescence Measurements for the pLas Promoters

Because I had constructed a transgenic strain of *E. coli* that was capable of expressing LuxR and LasR, it was now possible for me to test the functionality of the pLas' and pLasLux promoters that had been constructed over the summer. Constructs had been built previously that contained GFP downstream of the pLas' and pLasLux promoters (BBa_S03981 and BBa_S03984). I put these constructs into transgenic cells and non-transgenic cells. I also used wildtype MC4100 cells as a negative control and GFP producing construct (K091131) in HB101 as a positive control. Cells were exposed to a range of the different autoinducers in LB+antibiotic and fluorescence was measured after 20 hours of incubation at 37°C (Figure 23).

The two pLas promoters had very different responses to the various autoinducer inputs. pLas' demonstrated the expected expression pattern, as it was activated by 3OC12 and not induced by 3OC6. Additionally, the promoter was only activated in the transgenic MC4100 strain, providing further evidence that the LuxR/LasR expression cassette is in fact in the genome of the *E. coli*. The pLasLux promoter, however, appeared to be trasnscriptionally silent for all autoinducer inputs. One possible interpretation of these results is that, contrary to what we found in the literature (Waters and Bassler, 2005), 3OC12 was able to bind to both of the modified *las* and *lux* boxes (with the help of either LuxR or LasR). This one-way cross-reactivity could have repressed the pLasLux promoter at the *lux* box when only 3OC12 was supplied to the cells.

To test if cross reactivity existed between 3OC12 and the lux system, I utilized two existing constructs, the Lux Receiver (BBa_K09100) and Las Receiver (BBa_K091134). These constructs express LuxR and LasR respectively (when activated with IPTG) and also contain their respective wild-type promoter upstream of a GFP expression cassette (Figure 24). I exposed each of these receiver constructs (and controls) to all autoinducer treatments and
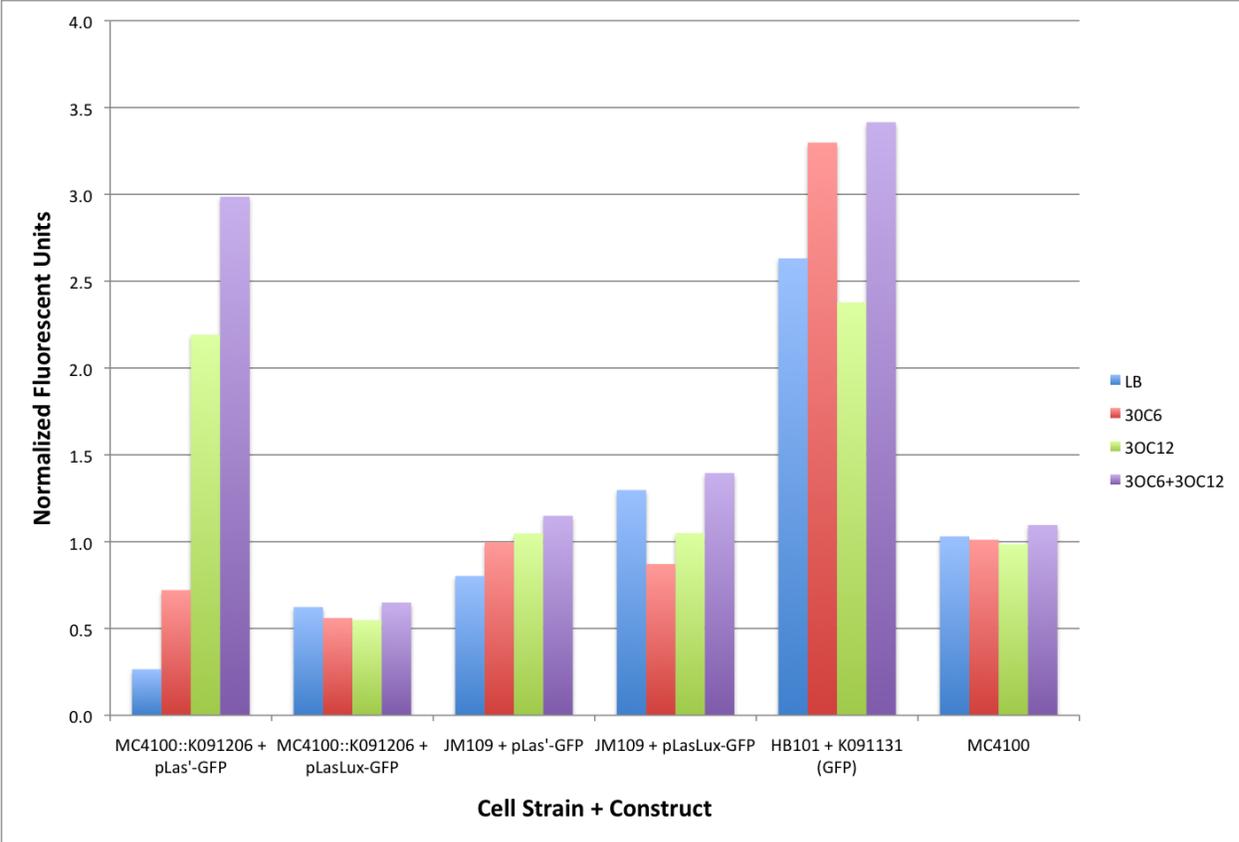
Figure 23: GFP expression of pLas' and pLasLux promoters based on variable autoinducer inputs. All data has been normalized to the average fluorescence of the negative control, MC4100. Autoinducer was supplied at a concentration of 10^{-5} M. Note that the expression of pLas' varied with different autoinducer inputs, while pLasLux was never activated.

observed GFP fluorescence (Figure 25). The Lux Receiver showed induction by both 3OC12 and 3OC6, while the Las Receiver was never activated. It should be noted that the Las Receiver has never been shown to function under any circumstances, so these results should be interpreted cautiously. Expression of the Lux Receiver was also more than 4 times greater when activated than was pLas' (note the difference in the scale of the y-axis between Figs 23 and 25).

(a) Lux Receiver
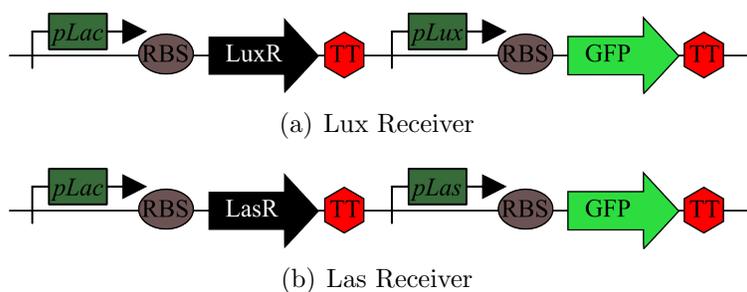
(b) Las Receiver

Figure 24: Design of the Lux Receiver (top) and Las Receiver (bottom). Receivers are designed to fluoresce when exposed to the proper autoinducer molecule.

I performed a final fluorescence experiment to verify that cells expressing LuxI and LasI were able to make and secrete their respective autoinducer molecule. To do this, I compared the GFP response of the Lux Receiver to autoinducer inducer inputs from two sources: purified autoinducer (AHL) and AHL sender cells (Figure 26). Sender cells contained previously constructed parts (S03608 and K091136) that constitutively expressed either LuxI or LasI. It was expected that these cells could synthesize AHL molecules that would be secreted into the media and absorbed by the Lux Receiver cells. My results showed that while the Lux Receiver's response to purified AHL was much more robust than the response to the sender cells, all autoinducer sources produced some type of increase in fluorescence. Again, we observed cross-reactivity between 3OC12 and the *lux* system. These results suggest that both the Las Sender and Lux Sender are functional to some extent.
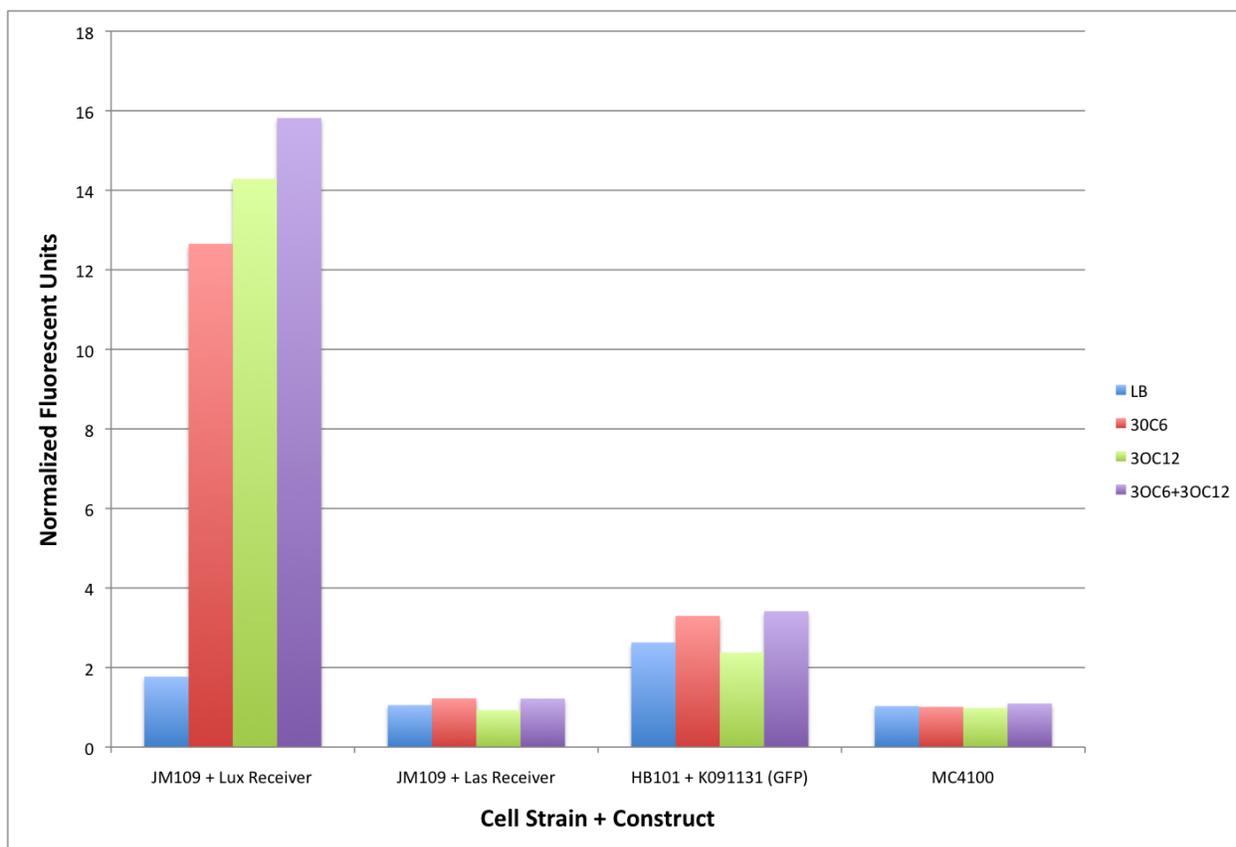
Figure 25: GFP expression of the Lux and Las Receivers based on variable autoinducer inputs. All data has been normalized to the average fluorescence of the negative control, MC4100. Autoinducer was supplied at a concentration of 10^{-5} M and the two receivers were also supplied with IPTG at 0.6ug/mL. Note that the expression of the Lux Receiver is induced by both 3OC6 and 3OC12.
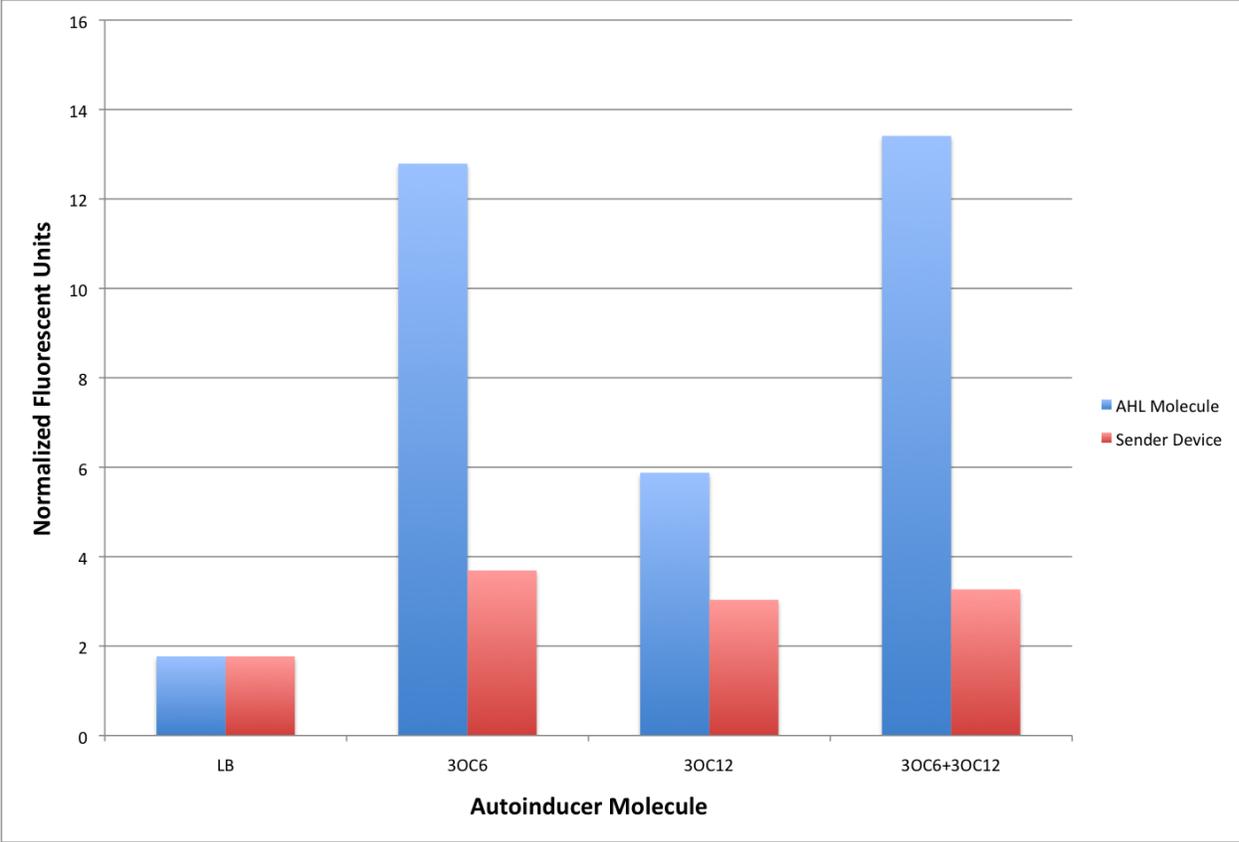
Figure 26: Comparison of fluorescent output of Lux Receiver when activated with AHL from two different sources. Response to purified 3OC6 and 3OC12 is shown in blue. Response to Lux and Las Sender cells is shown in red. Autoinducer was supplied at a concentration of 10^{-6} M.

Measuring Time-delayed Growth

In addition to my work building the XOR device, I also worked on testing and modeling a system for time-delayed growth using beta-lactamase diffusion. I first created a movie of time-delayed growth using time-lapse photography to prove the feasibility of this approach; the movie is available online

(`http://www.bio.davidson.edu/courses/genomics/2008/DeLoache/`

`TimeDelayedAmpRDiffusionWithTimes.avi`).

I have included some images from the movie below (Figure 27).

Figure 27: Time-delayed growth of colonies on an LB agar plate containing ampicillin (100 ug/mL). A colony expressing beta-lactamase was spotted at the top right corner of the frame. Non-ampicillin resistant colonies were then spotted in three linear paths away from the central colony. Growth occurs as the beta lactamase diffuses through the agar to neighboring colonies.

Having shown that time-delayed growth of colonies was possible with this system, I attempted to characterize further the properties that determined the rate of delayed colony growth. Modeling the system would make it possible to adjust different variables to regulate the time-delayed growth rate to the needs of a particular experiment. Therefore, I measured the growth rate of colonies as a function of ampicillin concentration, agar concentration, and temperature. Each growth condition was tested in triplicate and images were taken at various time intervals (Figure 28). I measured the distance from the front edge of the ampicillin-resistant colony to the nearest edge of the farthest non-resistant colony. Distances were plotted on graphs only if they were non-zero.
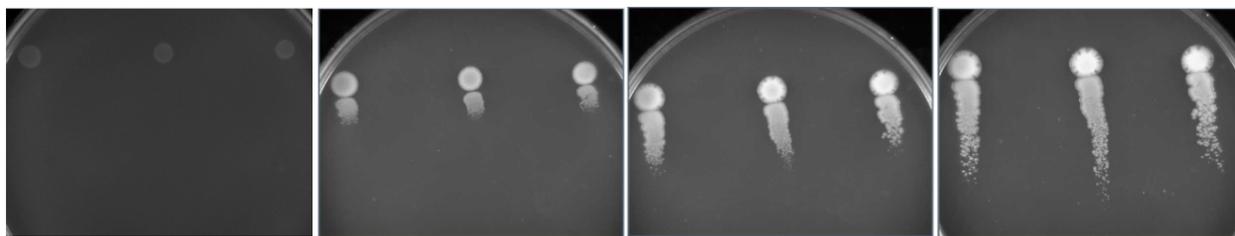
Figure 28: Sample images from the time-delayed growth experiment. Each panel contains an image of the 50 ug/mL ampicillin plate with 1.0X agar at various time points. Time points are, from left to right, 4 hours, 24 hours, 48 hours, and 72 hours.

As was expected, lower ampicillin concentrations yielded faster growth rates for all concentrations of agar (Figure 29). Somewhat surprisingly, the growth rate remained fairly constant throughout the 3 days of experimentation. Therefore, linear regression lines were drawn to estimate the rate of colony growth for each amp concentration at both temperatures (Figure 30 and 31). Looking at the slope of these regression lines, one can see that growth rate varies more between 25 and 50 ug/mL of ampicillin than it does between 50 and 100 ug/mL. This non-proportional difference suggests that colonies are more sensitive to changes in ampicillin concentration when the overall concentration of ampicillin is low.

The effect of agar concentration on growth rates gave unexpected results. I thought that higher agar concentrations would lead to slower growth rates because the beta lactamase would be slower to diffuse in these plates. However, my results actually showed the opposite effect (Figure 29). Notice that an agar concentration of 0.5X (triangles) always yields the slowest growth rate for a set ampicillin concentration.

A final interesting observation was the effect of temperature. Temperature had a greater impact for lower concentrations of ampicillin (Figures 30 and 31). At 100 ug/mL of ampicillin, the colony growth rate was essentially identical between 30°C and 37°C, though slightly higher at 30°C. However at 25 ug/mL of ampicillin, the growth rate was about 1.5 times higher at 37°C than it was at 30°C.
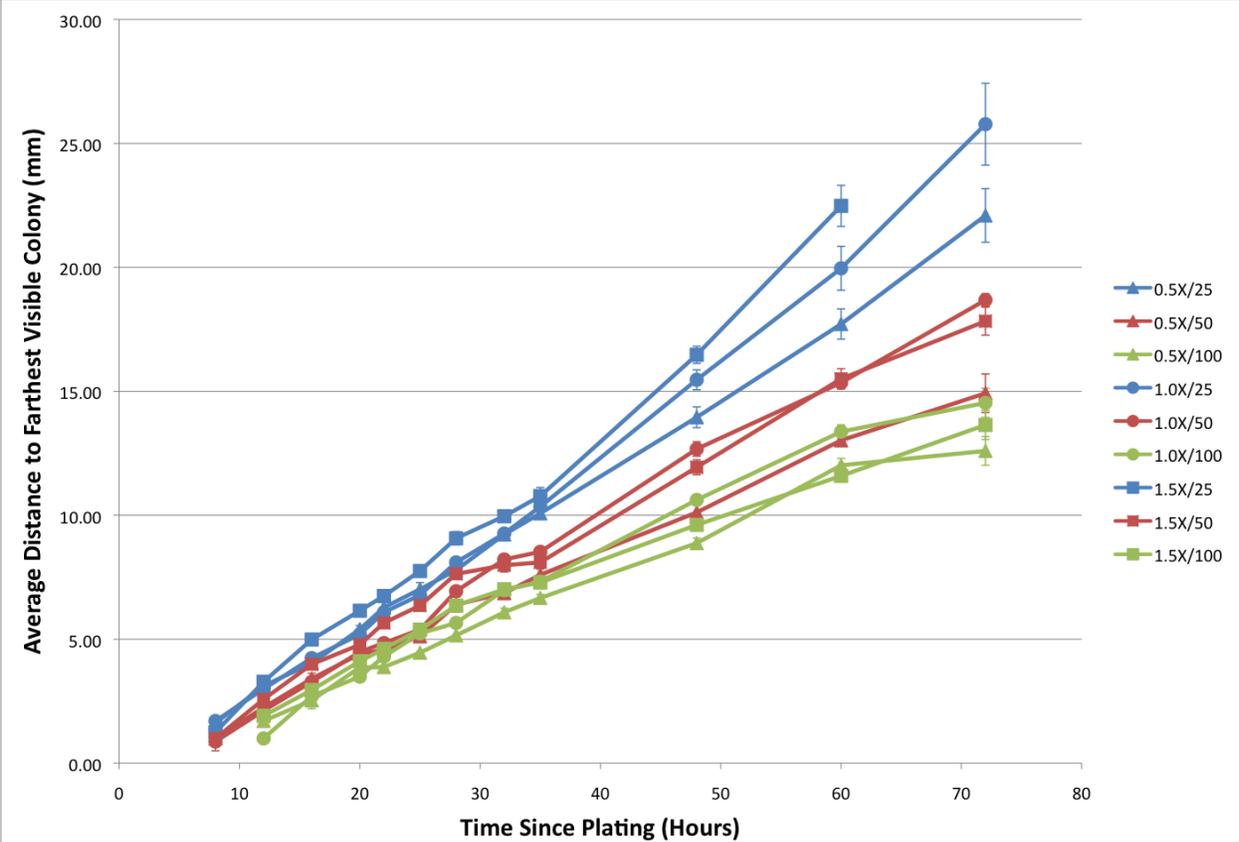
Figure 29: Distance of non-resistant colony growth over time for varying ampicillin and agar concentrations at 37°C. Legend values (i.e. 0.5X/25) represent agar concentrations (0.5X = 7.75g/L) and ampicillin concentrations (25 = 25ug/mL) respectively. Error bars represent 1 standard error from the mean. The last data point for the 0.5X/25 plate was tossed out because the agar on the plate dried and cracked during the final time interval.
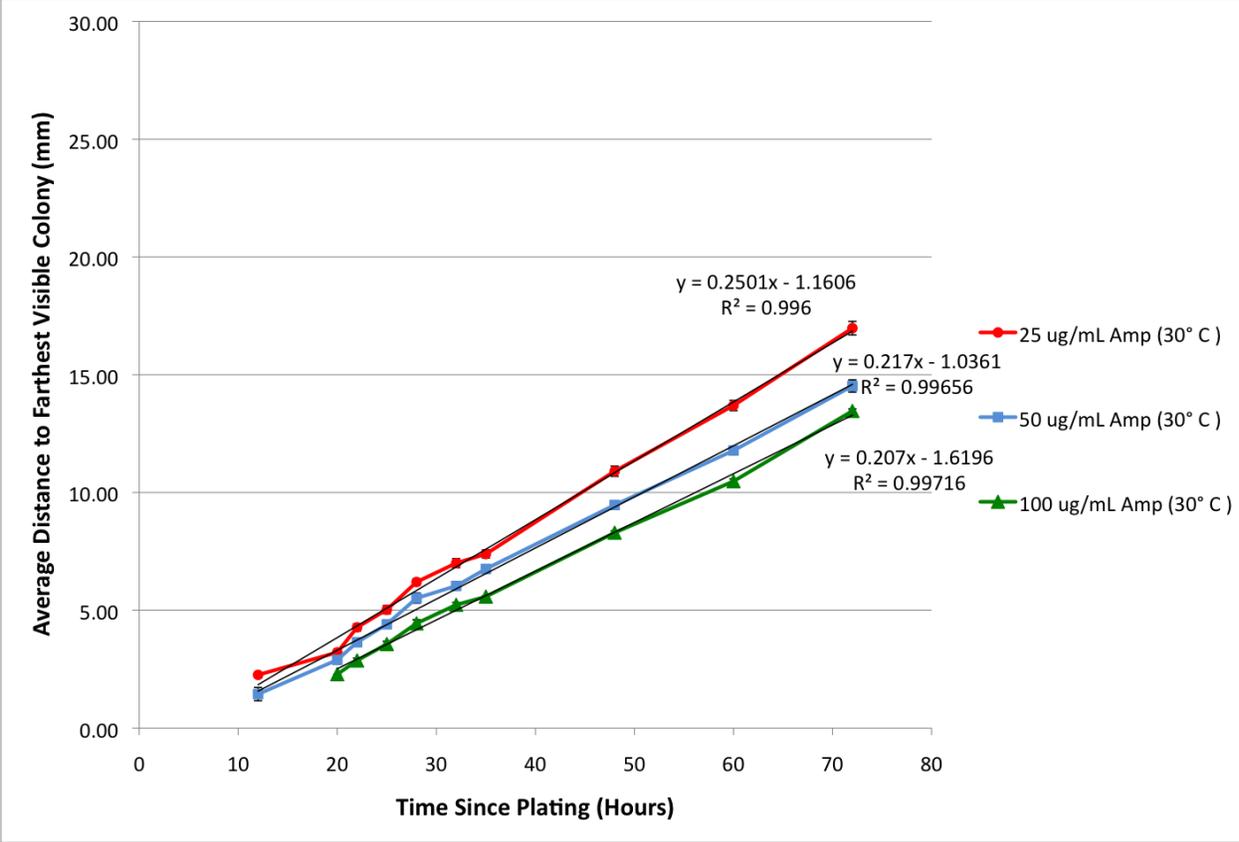
Figure 30: Distance of non-resistant colony growth over time for varying ampicillin concentrations at 30°C. Error bars represent 1 standard error from the mean. Linear regressions for each concentration are displayed with R-squared values.
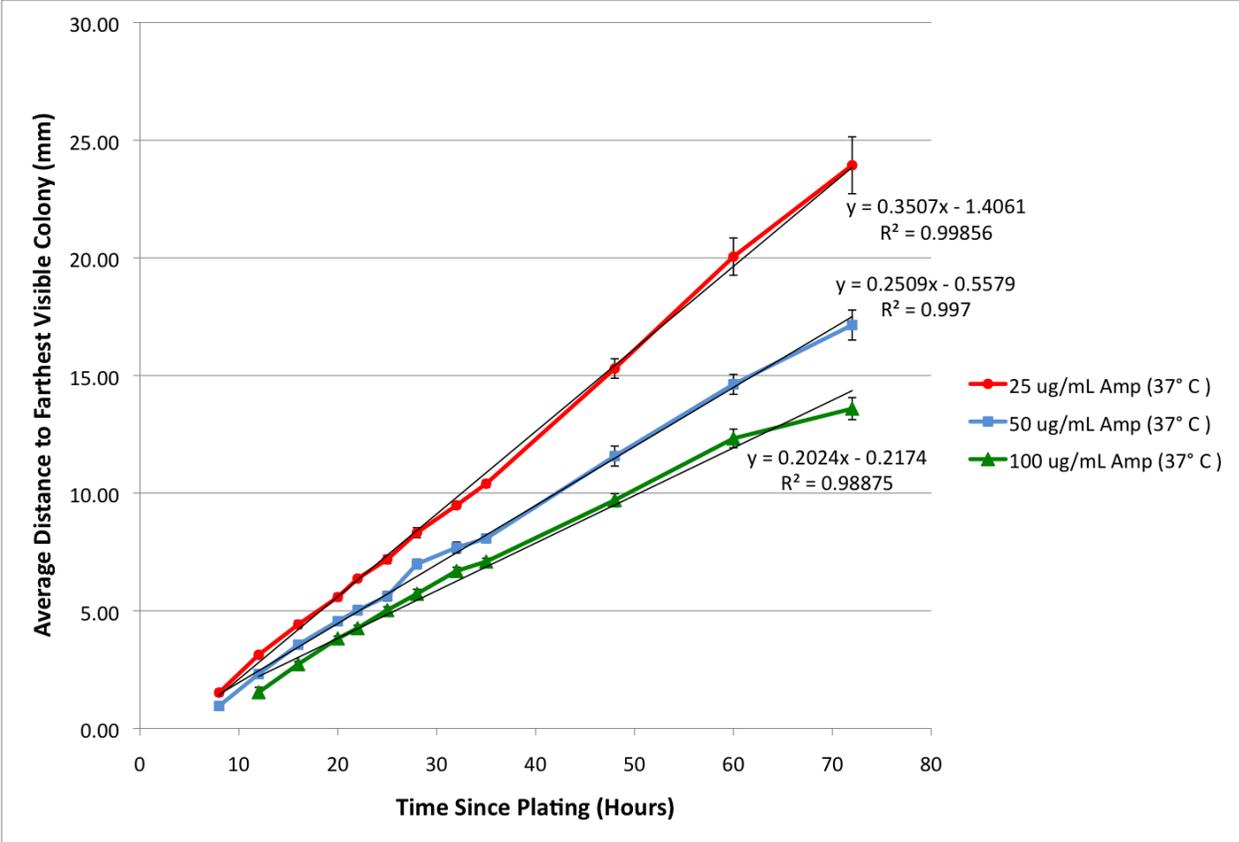
Figure 31: Distance of non-resistant colony growth over time for varying ampicillin concentrations at 37°C. Error bars represent 1 standard error from the mean. Linear regressions for each concentration are displayed with R-squared values.

Discussion

The construction of an *in vivo* XOR gate poses a significant challenge for synthetically constructed circuits. Due to its inherent properties, XOR logic requires a cell to respond differently to an input based solely on the presence or absence of a second input. The *lux* and *las* systems appeared to be good candidates for addressing this technical challenge for two reasons. The systems are similar enough that the design of our logic gate could be relatively simple. When dealing with something as complicated as biological systems, minimizing design complexity is necessary in order to reduce the probability of failure (Campbell and Heyer, 2007). Similarities between the *lux* and *las* systems allowed the design of the gate to consist of two mirrored halves that each rely on the same binding events. Additionally, while the *lux* and *las* systems are similar in function, Waters and Bassler (2005) showed the two systems are highly specific. Specificity prevents the components from interacting in an undesirable fashion.

Similarities and specificity made the *lux* and *las* systems good candidates for an XOR gate design, however, as is often the case in synthetic biology, the results of my experiments suggest that our understanding of the two quorum sensing systems is incomplete or wrong. The fluorescence data I collected indicate that LuxR can be activated by 3OC6 and 3OC12; both molecules activated the Lux Receiver. It should be noted here that the high level of activation in the Lux Receiver is probably due to the high copy number of *luxR* carried on a high copy plasmid inside those cells. The MC4100::K091206 transgenic strain has many fewer copies of *luxR* which could result in differences in the level of activation.

In addition to the Lux Receiver being activated by both autoinducers, the pLasLux promoter was not activated by 3OC12 as expected, while the pLas' promoter was. The simplest explanation for this behavior is that activated LuxR bound to the *lux* box in the -35 to -10 region and repressing the pLasLux promoter. If this hypothesis were true, then our

assumption that repression would override activation in a doubly bound promoter appears to be correct, but LuxR cross-reactivity has presented a whole new set of problems.

Waters and Bassler have claimed that different LuxR-type proteins possess binding pockets that only allow activation by the corresponding AHL molecule. However, my data suggests that there is perhaps more to be understood about specificity amongst quorum sensing systems. More experiments should be done to test cross-reactivity between 3OC12 and LuxR, though Kin Lau, working on a related project in the lab, has independently validated my results (personal communication).

If 3OC12 activates LuxR, then various approaches could be taken to modify the design of the XOR gate. Using a different set of quorum sensing systems that have less chance of cross-reacting would be one option. AHL molecules with very dissimilar structures might be a good starting point for that redesign (see: Parts Registry, Cell-Cell Signaling). Another option might be to mutate LuxR so that it is only activated by 3OC6. A third option might be to perform mutagenesis on the promoters themselves. If the 3OC12-bound LuxR has a different tertiary structure than 3OC6-bound LuxR, then perhaps it would be possible to generate a modified *lux* box that could only be bound by a 3OC6/LuxR complex but not 3OC12/LuxR. Regardless of which redesign pursued, potential cross reactivity between LuxR and 3OC12 poses a significant hurdle in the construction of a functional XOR gate. Further research must be done into the feasibility of various alternative approaches for fixing the system.

Another significant issue that I encountered was the cloning of the pLux' and pLuxLas promoters. After more than 8 months of attempts to ligate the <100 bp DNA fragments into a standard BioBrick plasmid, I have become convinced that the promoters may be in some way toxic to the cell. Toxicity would cause successful clones to be negatively selected and would make cloning difficult or impossible. Toxicity of the promoters is consistent with

my results throughout the year as well as results from the 2008 iGEM team. Primer dimer assembly resulted in at least 1 mutation in 100% of the sampled clones. Oligonucleotide assembly failed to give a product of the correct length multiple times. Finally, a relatively simple digestion and ligation of the synthesized promoters resulted in the cloning of an unidentified insert or a piece of genomic DNA. While my results might be the consequence of bad luck, the consistency of my inability to clone these two promoters leads me to conclude they are unclonable in their current form.

It is difficult to imagine a scenario where a basic promoter part could be toxic to the cell. One possibility is that the pLux' and pLuxLas promoters are binding a protein necessary for cell survival. It is also possible that the promoters are in some way interfering with the replication of the plasmid inside the cell. Still, it is difficult to explain how the pLux' promoter might be toxic to the cell, given that the sequence is so similar to the already-cloned wildtype pLux promoter.

In addition to the challenges I faced in cloning the pLux promoters, I had a lot of trouble getting the genomic insertion procedure to work correctly. Since I was the first student in the lab to try the procedure, there was a good bit of trial and error involved. My repeated attempts with HB101 cells were universally unsuccessful. After eliminating other possibilities, I concluded that the cell strain was the most likely reason for the failure. To demonstrate that cell strain was the problem, I performed the entire procedure on HB101 and MC4100 cells in parallel. MC4100 cells worked on the first attempt, while HB101 cells failed again. This parallel experiment is strong evidence that this genomic insertion procedure does not work in HB101 cells.

While I have investigated the possible reasons for HB101's behavior in a fair bit of depth, I have not found a suitable explanation. Haldimann and Wanner describe many different cell strains being used for their genomic insertion procedure. I had initially suspected that recA

might be the culprit since it is expressed in HB101 cells and is thought to be involved in suppressing recombination. However, some of the strains used by Haldimann and Wanner were *recA* positive, so recA probably is not the reason. It might be worth further investigation to determine why HB101 cells resist the insertion, however, in the meantime, they should never be used for the conditional replication insertion procedure.

After finally getting positive results for the genomic insertion procedure in MC4100, I verified insertion by PCR as described by Haldimann and Wanner. Based on the criteria they described, I convinced myself that I had isolated a transgenic strain with multiple copies of K091206 in the genome. However, some of my PCR results were not as I had predicted, so I ran a control PCR of pG80ko-K091206 miniprep using the same 4 primer combinations that were suggested by Haldimann and Wanner (1/4, 1/2, 3/4, and 2/3). Primers 2 and 3 bound to the pG80ko plasmid while primers 1 and 4 bound to the MC4100 genome. After a successful insertion, primers 1 and 4 are too far apart on the genome to give a product (as was seen on my gel for the transgenic MC4100).

I had expected to see a single band for the 2/3 primer combination, and no others. Instead I got products for all 4 primer combinations. The 1/4 band can be explained by the presence of genomic DNA in my miniprep that was amplified (not uncommon), however, it is more difficult to explain the other bands. Regardless, from the results of the fluorescence experiments in Figure 26, it is clear LuxR and LasR were expressed in the transgenic strain. Additional confirmation of a successful insertion could be obtained by sequencing the genomic DNA of the transgenic strain with primers 1 and 4.

The final portion of my thesis research focused on modeling the time-delayed growth system. Hopefully this work will assist the Davidson/MWSU team in the development of a bacterial hash function once a functional XOR gate is available. The time-delayed growth system could also be implemented in many other synthetic biology projects that require a signal to

be passed sequentially between cells. By better understanding the parameters that determine the rate of colony growth, it will easier to modify the components of the system to fit the needs of specific projects. While I only varied ampicillin concentration, agar concentration, and temperature, it would also be interesting to vary the copy number of the beta lactamase plasmid to control the rate of beta lactamase diffusion.

Aside from providing growth rates for different ampicillin concentrations at different temperatures (the slopes of the regression lines in Figures 30 and 31), the results that I obtained from my experiment showed some interesting and unexpected trends. Contrary to my intuition, increased agar concentration increased the growth rate of the colonies. I had expected to observe the opposite trend, so I performed a literature review to investigate the interaction between agar concentration and antibiotic efficiency. Toama *et al.* (1978) provide a possible explanation for my results. They reported that the efficiency of naficillin is decreased by increasing agar concentrations. The similar structures of naficillin and ampicillin make it possible that a similar agar interaction is occurring on ampicillin plates. If so, then increasing agar concentration would decrease the efficiency of the ampicillin in the plate and increase the rate of time-delayed colony growth.

Another unexpected result was the linearity of the growth curves for all growth conditions. Initially, I had expected to see a sigmoidal growth curve for non-ampicillin resistant colonies. I predicted that the ampicillin resistant colony would take a while to start producing beta lactamase. Once secretion of beta lactamase had ramped up, I expected to see colony growth leveled off, as the area available for diffusion got larger by a factor of the radius squared. However, it was difficult to find any significant amount of curvature in the data. Perhaps the time-delayed growth rate was affected by the exponential growth of the initial ampicillin resistant colony secreting beta lactamase more than expected (canceling out the increasing area). It is also possible that 3 days wasn't long enough to see reduction in the growth rate.

Regardless, the linear data made it easy to model time-delayed growth for each condition.

Finally, I also observed that temperature had a more significant effect on the growth rate of colonies in low ampicillin concentrations than in high ampicillin concentrations. Plates with an ampicillin concentration of 100 ug/mL showed no significant difference between the two temperature treatments, while 25 ug/mL ampicillin plates had much higher growth rates at 37°C than at 30°C. This result was contrary to my predicted behavior of all growth rates being higher at 37°C. One possible explanation for this finding is that the temperature affects the efficiency of the ampicillin, however, more testing would have to be done to investigate the reasons behind this result.

Before the XOR gate and time-delayed growth systems could be implemented to construct a physical bacterial hash function, more work needs to be done to redesign and construct functional XOR promoters. Based on the difficulty of cloning the pLuxLas promoter, and the 3OC12 repression of the pLasLux promoter, a mutagenesis screen may be required to develop functional promoters. Nevertheless, my project fulfilled both of the overarching goals of synthetic biology by exposed gaps in our understanding of biological principles and helping make progress towards a functional bacterial hash function.

Acknowledgements

References

C. M. Ajo-Franklin, D. A. Drubin, J. A. Eskin, E. P. S. Gee, D. Landgraf, I. Phillips, and P. A. Silver. Rational design of memory in eukaryotic cells. *Genes Dev*, 21(18):2271-2276, 2007. ISSN 0890-9369.

H. J. Anderson. Starting from scratch. *Health Data Manag*, 16(3):48, 2008 Mar.

J. C. Anderson, E. J. Clarke, A. P. Arkin, and C. A. Voigt. Environmentally controlled invasion of cancer cells by engineered bacteria. *J Mol Biol*, 355(4):619–627, 2006 Jan 27.

J C. Anderson, C. A. Voigt, and A. P. Arkin. Environmental signal integration by a modular and gate. *Mol Syst Biol*, 3:133, 2007. ISSN 1744-4292.

D. Baker, G. Church, J. Collins, D. Endy, J. Jacobson, J. Keasling, P. Modrich, C. Smolke, and R. Weiss. Engineering life: building a fab for biology. *Sci Am*, 294(6):44–51, 2006 Jun.

Brown University iGEM Team. Bacterial Freeze Tag. 2006. URL `http://parts.mit.edu/wiki/index.php/Brown:Bacterial_Freeze_Tag`

A. M. Campbell and L. J. Heyer. *Discovering Genomics, Proteomics, and Bioinformatics.* New York: Pearson Benjamin Cummings, 2007.

K. A. Egland and E. P. Greenberg. Conversion of the vibrio fischeri transcriptional activator, luxr, to a repressor. *J Bacteriol*, 182(3):805-811, 2000. ISSN 0021-9193.

M. B. Elowitz and S. Leibler. A synthetic oscillatory network of transcriptional regulators. *Nature*, 403(6767):335–338, 2000 Jan 20.

Davidson/MWSU iGEM. Hamiltonian path finders. 2007. URL `http://openwetware.org/wiki/Davidson:Davidson_Missouri_W`.

Davidson/MWSU iGEM. Math modeling pages. 2008. URL `http://gcat.davidson.edu/GcatWiki/index.php/Math_Modeling_Pages`.

D. Endy. Foundations for engineering biology. *Nature*, 438(7067):449-453, 2005. ISSN 1476-4687

D. Ferber. Synthetic biology. microbes made to order. *Science*, 303(5655):158–161, 2004.

T. S. Gardner, C. R. Cantor, and J. J. Collins. Construction of a genetic toggle switch in Escherichia coli. *Nature*, 403(6767):339-342, 2000. ISSN 0028-0836.

A. Haldimann and B. Wanner. Conditional-replication, integration, excision, and retrieval plasmid-host systems for gene structure-function studies of bacteria. *Journal of Bacteriology*, 183(21):6384–6393, 2001.

K. A. Haynes, M. L. Broderick, A. D. Brown, T. L. Butner, J. O. Dickson, W. L. Harden, L. H. Heard, E. L. Jessen, K. J. Malloy, B. J. Ogden, S. Rosemond, S. Simpson, E. Zwack, A. M. Campbell, T. T. Eckdahl, L. J. Heyer, and J. L. Poet. Engineering bacteria to solve the burnt pancake problem. *J Biol Eng*, 2(1):8, 2008. ISSN 1754-1611.

T. Knight. 2003. Standard Assembly: BioBrick Parts. URL `http://parts2.mit.edu/wiki/index.php/Standard_Assembly`.

B. P. Kramer and Martin Fussenegger. Hysteresis in a synthetic mammalian gene network. *Proc Natl Acad Sci USA*, 102(27):9517-9522, 2005. ISSN 0027-8424.

B. P. Kramer, Cornelius Fischer, and Martin Fussenegger. Biologic gates enable logical transcription control in mammalian cells. *Biotechnol Bioeng*, 87(4):478-484, 2004. ISSN 0006-3592.

D. Mackenzie. Computer science. cryptologists cook up some hash for new Òbake-offÓ. *Science*, 319(5869):1480-1481, 2008. ISSN 1095-9203.

MIT Parts Registry. Featured parts cell cell signaling. 2007. URL http://partsregistry.org/Featured_Parts:Cell-Cell-Signaling.

MIT Parts Registry. Part:BBa_F2620:Transfer Function. 2008 URL http://partsregistry.org/Part:BBa_F2620:Transfer_Function.

OpenWetWare. Ampicillin. URL `http://openwetware.org/wiki/Ampicillin`.

J. P. Pearson, K. M. Gray, L. Passador, K. D. Tucker, A. Eberhard, B. H. Iglewski, and E. P. Greenberg. Structure of the autoinducer required for expression of Pseudomonas aeruginosa virulence genes. *Proc Natl Acad Sci USA*, 91(1):197-201, 1994.

D.-K. Ro, E. M. Paradise, M. Ouellet, K. J. Fisher, K. L. Newman, J. M. Ndungu, K. A. Ho, R. A. Eachus, T. S. Ham, J. Kirby, M. C. Y. Chang, S. T. Withers, Y. Shiba, R. Sarpong, and J. D. Keasling. Production of the antimalarial drug precursor artemisinic acid in engineered yeast. *Nature*, 440(7086):940–943, 2006 Apr 13.

C. Tan, H. Song, J. Niemi, and L. You. A synthetic biology challenge: making cells compute. *Mol Biosyst*, 3(5):343-353, 2007. ISSN 1742-206X.

M. A. Toama, A. A. Issa, and M. S. Ashour. Effect of agar percentage, agar thickness, and medium constituents on antibiotics assay by disc diffusion method. *Die Pharmazie*, 33(2/3): 100-102, 1978.

C. M. Waters and B. L. Bassler. Quorum sensing: cell-to-cell communication in bacteria. *Annu Rev Cell Dev Biol*, 21:319-346, 2005. ISSN 1081-0706.

M. N. Win and C. D. Smolke. Higher-order cellular information processing with synthetic rna devices. *Science*, 322(5900):456–460, 2008.

C. Zimmer. 2006 scientist of the year: Jay Keasling. *Discover*. (December)34-37, 2006.